Non-POU Domain-Containing Octomer-Binding (NONO) protein expression and stability promotes the tumorigenicity and activation of Akt/MAPK/β-catenin pathways in human breast cancer cell Running title: NONO promotes the tumorigenicity of breast cancer

Bilal Ahmad Lone
South Asian University
Fouzia Siraj
National Institute of Pathology, Safdarjung Hospital Campus, Room No.610, 6th Floor, Ansari Nagar, New Delhi, 110029, India
Ira Sharma
National Institute of Pathology, Safdarjung Hospital Campus, Room No.610, 6th Floor, Ansari Nagar, New Delhi, 110029, India
Shweta Verma
CSIR-Institute of Genomics and Integrative Biology (CSIR-IGIB), New Delhi-110025, India
Shibendra Kumar Lal Karna
South Asian University
Faiz Ahmad
South Asian University
Preeti Nagar
South Asian University
Chetana Sachidanandan
CSIR-Institute of Genomics and Integrative Biology (CSIR-IGIB), New Delhi-110025, India
Yuba Raj Pokharel (yrp@sau.ac.in)
South Asian University

Research Article

Keywords: Breast cancer, NONO, Pin1, MAPK/β-catenin, P53, Metastasis, Apoptosis, Cancer Stem Cells

Posted Date: December 8th, 2022

DOI: https://doi.org/10.21203/rs.3.rs-2319552/v1

Abstract

Breast cancer is one of the most common cancers with high mortality, highlighting the vital need to identify new therapeutic targets. Here we report that Non-POU Domain-Containing Octamer-Binding (NONO) Protein is overexpressed in breast cancers and validated the interaction of WW domain of PIN1 with c-terminal Threonine-Proline (thr-pro) motifs of NONO. The interaction of NONO with PIN1 enhances NONO's stability by inhibiting its proteasomal degradation, and this identifies PIN1 as a positive regulator of NONO to promote breast tumor development. Functionally, silencing of NONO inhibits the growth, survival, migration and invasion, epithelial-to-mesenchymal transition (EMT), and stemness of breast cancer cells in vitro. A human metastatic breast cancer cell xenograft was established in transparent zebrafish (Danio rerio) embryos to study the metastasis inability of NONO silenced breast cancer cells in vivo. Biochemical analysis indicated NONO as a master regulator of the molecules associated with different hallmarks of cancer. Mechanistically, depletion of NONO promotes the expression of PDL1 cell surface protein in breast cancer cells. The identification of novel interactions of NONO with c-Jun and β-catenin proteins and activating the Akt/MAPK/β-catenin signalling suggests NONO as novel regulator of Akt/MAPK/β-catenin signalling pathways. Taken together, our results demonstrated an essential role of NONO in the tumorigenicity of breast cancer and could be a potential target for anti-cancerous drugs.

Background

Breast cancer is the most common type of cancer diagnosed worldwide, with an estimated 2.3 million new cases [1]. It has a high recurrence rate as well as tendency to metastasize which serves the pathological condtions [2]. Once metastasize, the cancer cells develop stemness and becomes more resistant to apoptosis and thus the treatment becomes more challenging [3][4]. Therapeutic strategies of breast cancer have significantly improved; however, the patients with distant metastatic breast cancer are less responsive to the standard treatment. Although targets like Her2, ER or PR has been promising molecules in treating certain breast carcinoma, there remains need to explore the role of other proteins and dissect their molecular mechanism in breast carcinogenesis for understanding the disease and develop effective targeted therapies for breast cancer patients.

The NONO, also known as 54 kD nuclear RNA- and DNA-binding protein (p54nrb), is a multifunctional DBHS (Drosophila behavior/human splicing) protein defined by N-terminal RNA recognition motifs (RRMs), protein-protein interaction NONA/paraspeckle domain (NOPS), and a C-terminal coiled-coil domain [5][6] binds DNA, RNA, and proteins [5]. The NONO protein is primarily found in the nucleus, especially in paraspeckles [7], and is involved in every step of gene regulation: transcriptional activation and repression [8], termination of transcription [8], pre-mRNA splicing [8], RNA transport [9] as well as nuclear retention of defective RNA for editing [10]. It has been demonstrated that the interaction of NONO with splicing factor proline and glutamine-rich (SFPQ) regulates DNA repairing [11]. Because NONO plays important role in multiple processes, it is dysregulated in many cancers. In breast cancer, the expression of NONO promotes the transcriptional activation of lipogenic genes and lipid production by interacting with and stabilizing the sterol regulatory element-binding protein 1 (SREBP1) [12]. Modulation of EGFR

and STAT3 stabilization by NONO exerts the oncogenic behaviour, chemotherapy resistance and poor prognosis in triple-negative breast cancer (TNBC) patients [13][14]. Additionally, NONO promotes the growth of breast cancer cells by regulating the posttranscriptional expression of S-phase-associated kinase 2 and the E2F transcription factor [15]. In hepatocarcinoma, NONO contributes to carcinogenesis through the oncogenic splicing of BIN1 protein. NONO is strongly expressed in prostate cancers and promotes castration-resistant prostate cancer development by causing differential EPHA6 splicing [16] [17]. Furthermore, NONO expression is significantly elevated in melanoma [18] gastric cancer cells [19], and Esophageal squamous cell carcinoma [20], and the increased expression of NONO is associated with the aggressiveness of cancers.

Proline (Pro)-directed serine or threonine (Ser/Thr-Pro) phosphorylation (pSer/Thr-Pro) is a typical signalling mechanism in cell proliferation and transformation [21]. Peptidyl-prolyl cis-trans isomerase NIMA-interacting 1 (PIN1) regulates the conformational changes of pSer/Thr-Pro motifs and causes the change in the structure, function, or stability of numerous proteins [22][23]. PIN1 is commonly dysregulated in various cancer, and overexpression and/or overactivation is linked to a poor clinical prognosis [24], [25]. It has been demonstrated that overexpression of PIN1 accelerates genomic instability and promotes tumorigenesis by disrupting cell cycle coordination [26]. Ablation of PIN1 effectively suppresses the tumor development in Neu or Ras transgenic mice [27]. Over-activation of PIN1 disrupts the balance between oncogenic and tumor-suppressing proteins, moving it towards oncogenesis; more than 40 oncogenes are activated, and over 20 tumor suppressors are inactivated in numerous cancers [21]. PIN1 significantly contributes in oncogenesis with its ability to stabilize oncoproteins and destabilize tumor suppressors [21]. In our previous study we used web-based protein interaction network analysis platform called relevance rank platform (RRP) to predicted functional relevance between the PIN1 oncoprotein and NONO [28] however, the detailed mechanism by which PIN1 modulates NONO activity and promotes NONO-induces cell proliferation and transformation remains unclear.

Many gene regulators that drive oncogenesis are regulated by PIN1 [29], and NONO has recently emerged as a key regulator in cancer development[15]. NONO harbors multiple Thr-Pro motifs, this prompted us to explore whether PIN1 is a positive regulator of NONO. Our study have revealed that threonine (T)428 and T450 specifically binds with the WW domain of PIN1. Binding of PIN1 promotes the stability and abundance of NONO, and promotes NONO induced activation of downstream signalling pathway involved in cancer development. Our results uncover the role and molecular mechanism by which NONO contributes to the development of breast cancer. Giving its crucial role in activating Akt/MAPK/β-catenin signalling, NONO might be a potential therapeutic target for breast cancer.

Materials And Methods

Cell culture, antibodies and reagents.

MDA-MB-231 and MCF-7 cells were purchased from NCCS Cell Repository (Pune, India) and maintained in DMEM medium supplemented with 10% FBS, 100 units/ml penicillin (all from Gibco, ThermoFisher

Scientific, USA) at 37°C and 5% CO2. Antibodies against NONO, PIN-1, β-catenin, Bax, Bcl-xl, Caspase-3, pP38, Cyclin E1, eIF4E, RACK1, NF-kB, and pNF-kB were purchased from Santa Cruz Biotechnology (Dallas, Texas, USA). The antibodies against PCNA, Vimentin, MMP-2, MMP-9, P53, and E-cadherin were purchased from Cloud-Clone Corp (Houston, USA). The antibodies against c-Jun and pc-Jun antibodies were purchased from Cell Signaling Technology. The antibodies against β-actin and p-P53 and MG132 were purchased from SigmaAldrich. Matrigel was purchased from Corning Incorporated Lifescience (Tewksbury, MA, USA).

Zebrafish lines and maintenance

Zebrafish (Danio rerio) were bred, raised and maintained at 28.5 °C under standard conditions as described [30]. To prevent the pigment formation for fluorescence imaging, embryos older than 24hpf were raised in embryo medium containing 0.003% phenylthiourea. Zebrafish handling was in strict accordance with good animal practices as described by the Committee for the Purpose of Control and Supervision of Experiments on Animals (CPCSEA), Government of India. All the experiments were approved by The Institutional Animal Ethics Committee (IAEC) of the CSIR-Institute of Genomics and Integrative Biology, New Delhi, India.

Transfection of siRNAs

Using Lipofectamine RNAiMAX (ThermoFisher Scientific), cells were transiently transfected with oligo siRNAs (FlexiTube siRNA, QIAGEN) following the manufacturer's directions. Table 1 lists the siRNA sequences used in this study.

Table 1 Sequence of siRNAs

siRNA	Scramble (scr)	NONO
Target (5'-3')	AATTCTCCGAACGTGTCACGT	AGGCTTGACTATTGACCTGAA
sense (5'-3')	UUCUCCGAACGUGUCACGUdTdT	GCUUGACUAUUGACCUGAATT
Antisense(5'-3')	ACGUGAGACACGUUCGGAGAAdTdT	UUCAGGUCAAUAGUCAAGCCT

Cell cycle

The distribution of the cell population in the different stages of the cell cycle was investigated using siRNA-scr and siRNA-NONO transfected MDA-MB-231 and MCF-7 cells. Cells were collected and washed with PBS after a 72-hours transfection. After that, the cells were fixed in 70% cooled ethanol and kept at 4°C overnight. The next day the cells were centrifuged, ethanol was removed, and two PBS washes were performed. After that, the cells were incubated with RNase (10 µg/mL) and Propidium iodide (25 µg/mL) and maintained at 37°C for 30 minutes. FACS verse was used to evaluate the samples. Each sample had 10,000 events, and the data were analysed with ModFit LT software.

Colony formation assay

Following transfection with siRNA-scr and siRNA-NONO, MDA-MB-231 and MCF-7 cells were evaluated to form colonies. 5 X 10^2 cells from the scramble and NONO knockdown cells were plated in each well after the cells had been transfected for 24 hrs. The culture was retained for 12 days, and the media was replaced every 48 hours. The cells were fixed using methanol and stained with 0.4 percent crystal violet. Image J software was used to count the colonies.

Wound healing assay

In each well of a six-well plate, 4 x10^5 MDA-MB-231 and MCF-7 cells were seeded and transfected with siRNA-scr and siRNA-NONO. A scratch was delivered with a 200 ul pipette tip once the monolayer had formed. Detached cells were removed after washing the cells. Then, images of the wound region were captured at different time intervals. Analysis was performed using ImageJ. After normalization of the wound area, the % wound healed area was calculated.

Migration and invasion assay

To evaluate migration and invasion potential of breast cancer cells, 8 µm pore size Transwell chambers (Corning) were placed in a 24 well plate. The 24-hour post-transfection cells (4 X10^4) were plated in 200 µl of serum-free medium for the migration test. At the same time, the bottom chamber was filled with 700 µl of 10% serum-supplemented media, a source of chemoattractant. The invasion experiment was performed in the same way except the upper chamber was evenly covered with 80 µg Matrigel (Corning) diluted in 100 µl DMEM and incubated at 37°C for 2 hours. The cells were suspended in chambers and incubated for 48 hours at 37°C with 5% CO2. The cells were then fixed using methanol and stained with 0.4 percent crystal violet.

In-vivo assay for metastasis analysis in zebrafish embryos

2dpf (days post fertilization) Tubingen wild type zebrafish embryos were dechorionated and then anesthetized using 0.015M tricaine (Sigma-Aldrich, Cat. No. A5040). Embryos were then aligned on a flat 2% agarose plate in lateral position. To investigate the effect of NONO knockdown on metastasis potential of MDA-MB-231 cells, embryos were injected with approximately equal number of (45-150) Green CM-FDA labelled cells into the perivitelline space. Then embryos were collected and maintained in 1-phenyl-2-thiourea (0.003% in Embryo medium) containing (Sigma-Aldrich, Cat. No. P7629) at 28°C. Embryos were imaged at 72 hpi (hours post injections) using Nikon Eclipse Ti or Zeiss AxioScope A1 microscopes.

RNA isolation and quantitative PCR

TRIzol reagent (ThermoFisher Scientific, Inc.) was used to isolate total RNA from the siRNA-scr and siRNA-NONO transfected MDA-MB-231 and MCF-7 cells. The cDNA was prepared from 2µg of total RNA according to the manufacturer's instructions (ThermoFisher Scientific, Inc.). Table 2 lists the primers used

against the genes under investigation. The PCR cycling schedule was 10 minutes at 95°C, followed by 40 cycles of 15 seconds at 95°C, 30 seconds at 60°C, and a melt curve with a single reaction cycle at 95°C for 15 seconds, 60°C for 1 minute, and dissociation at 95°C for 15 seconds. The resulting Ct values were then normalized with reference to the quantification of housekeeping gene GAPDH. The relative expression of genes was determined using the $2^{-\Delta\Delta Ct}$ method.

Table 2. List of primers used for Real-Time PCR

GENE	FORWARD PRIMER SEQUENCE	REVERSE PRIMER SEQUENCE
NONO	5'- GGAGCCCATGGACCAGTTAG-3'	5'- AAATCTGGGTGGCTGCTCTC-3'
PIN1	5'- TTTGAAGACGCCTCGTTTGC-3'	5'-GTGCGGAGGATGATGTGGAT-3'
p21	5'-CTGCCCAAGCTCTACCTTCC-3'	5'-CGAGGCACAAAGGGTACAAGA-3'
GAPDH	5'-GTCAAGGCTGAGAACGGGAA-3'	5'-AGTGGCTCCATTCACCGC-3'
OCT4	5'-GAGAACCGAGTGAGAGGCAAC-3'	5'- CTGATCTGCTGCAGTGTGGGT-3’
SOX2	5'-TTTGTCGGAGACGGAGAAGC-3'	5'-TAACTGTCCATGCGCTGGTT -3'
Slug	5'-ACTCACTCGCCCCAAAGATG-3'	5'-TCTCTCCTCTTCCTTCCTCCAT-3'
Twist	5'-CTCGGACAAGCTGAGCAAGA-3'	5'-GCTCTGGAGGACCTGGTAGA-3'
Cyclin E1	5'-ATACTTGCTGCTTCGGCCTT-3'	5'- TCAGTTTTGAGCTCCCCGTC-3'

Crystal violet assay

Crystal violet assay was used to determine the viability of NONO-depleted breast cancer cells. MDA-MB-231 and MCF-7 cells were transfected with a scramble and NONO siRNAs in a six-well plate and incubated for 24 hours. The cells were then harvested and counted, and $5X10^3$ cells were planted into each well of a 96-well plate and incubated at 37 ˚C, 5% CO_2 for next 48 hours. After that, the medium was removed, and the cells were stained for 30 minutes with 0.4 percent crystal violet (prepared in 50 percent methanol). The wells were then cleansed with water to remove any remaining discoloration and air-dried for 12 hours. The next day, the dye was dissolved in 100 µL of methanol, and the absorbance of the dissolved dye was measured at 570 nm. The viability of siRNA NONO w.r.t. siRNA scramble was determined as fold change absorbance value.

JC1 staining and flow cytometry

The impact of the silence of NONO on mitochondrial membrane potential was assessed with the fluorescent JC-1 dye using flow cytometer. MDA-MB-231 and MCF-7 scrambled, and siRNA-NONO transfected cells were incubated at 37˚C, 5% CO2 for 48 hours. Following that, the cells were harvested and stained with JC-1 dye for 30 minutes in the dark. Cells were then collected, washed with PBS, and fluorescence was analyzed by flow cytometry (FACS Verse, BD).

Flow cytometry-based detection of the intracellular ROS

Following the knockdown of NONO, we examined intracellular reactive oxygen species (ROS) in MDA-MB-231 and MCF-7 cells. After 48 hours of transfection, the cells were trypsinized and resuspended in PBS with MitoSOX^{TM} Red (Thermo Scientific) at a final concentration of 5 µM. The levels of intracellular ROS were measured using Flow cytometry.

Preparation of total cell lysate and western blot analysis

The preparation of total cell lysates and the analysis of western blots were carried out as described previously [31]. Electrophoresis of an equivalent amount of cell lysate (30 µg) on 6~15% percent SDS-PAGE gels was performed, followed by electrotransfer to a PVDF membrane. As directed by the manufacturer, individual proteins were detected with an ECL Western Blotting Kit (Bio-Rad). ImageJ software was used for densitometry, and the density of the protein of interest was normalized to that of β-actin using arbitrary densitometric units.

Flow cytometric analysis of apoptosis

Annexin V-FITC and Propidium iodide staining assay and FACS verse analysis (BD) were used to investigate the effect of silencing of NONO on apoptosis. Breast cancer cells were transfected with the siRNA-scramble and siRNA-NONO and incubated for 72 hours at 37˚C, 5% CO2. The cells were then harvested and incubated for 30 minutes with a 1X binding buffer containing Annexin V and Propidium iodide. Following this, the samples were collected for FACS analysis (BD).

Lentiviral CRISPR construct generation

The guide sequences targeting two distinct regions of the human *NONO* gene were designed as described previously [32]. Guide oligonucleotides containing the BsmBI restriction site overhangs were annealed and cloned into BsmBI linearized LentiCRISPRv2 vector for the current study following previously published protocol [33]. Correct insertion of guide sequence was confirmed using Sanger sequencing. The oligo sequences for sgRNA cloning are listed in Table 3.

Table 3. The oligo sequencing for sgRNA cloning used in the study

gRNA oligonucleotides		
sgRNAs	gRNA oligos	Sequence (5'-3')
NONO gRNA1	F	CACCGCAATCCGTTCGACGACGACG
	R	AAACCGTCGTCGTCGAACGGATTGC
NONO gRNA2	F	CACCGCCTAGCGGAGATTGCCAAAG
	R	AAACCTTTGGCAATCTCCGCTAGGC
Scramble gRNA	F	CACCGAAACGGCGGATTGACCGTAA
	R	AAACTTACGGTCAATCCGCCGTTTC

Lentivirus production and infection.

Lentivirus particles were generated by co-transfection of 2 µg transfer plasmid LentiCRISPRv2 (Addgene #52961) or pLJM1-EGFP (Addgene #19319: positive control) with 1.5 µg packaging plasmid psPAX.2 (Addgene #12260) and 0.5 µg envelop plasmid pCMV-VSV-G (Addgene #8454) in a single well of a six-well plate of 80% confluent HEK-293T cells using 12 µl of Effectene transfection reagent (QIAGEN). After 12 hours of transfection, the media was changed to complete DMEM. The virus-containing culture media was harvested and centrifuged at 3,000 rpm at 4˚C for 10 minutes after 48 hours of transfection. The collected supernatant was filtered with a 0.45 µm filter membrane and used immediately.

Lentivirus infection was performed by mixing the 1 ml cell suspension of $4x10^5$ cells and 1 ml polybrene (10 µg)/virus solution at a multiplicity of infection <1. The plate was centrifuged at 931 g for 45 minutes at 30˚C. After spinning, the cells were incubated at 37˚C overnight in a tissue culture incubator. The following day, cells were re-seeded in 10cm dishes at a density of 100-500 cells/plate. For antibiotic selection, the MDA-MB-231 and MCF-7 cells were treated with 2 µg/ml and 0.5 µg/ml of puromycin, respectively, after 48 hours of incubation. Cells were cultured in puromycin media for 4-5 days until the death of all the control cells. The cells were further grown until single colonies were visible. The colonies were then picked up manually for single clone expansion. Some surviving colonies in both cell lines are negative for NONO expression. Knockout of the *NONO* gene was then verified by western blotting.

Yeast two-hybrid (Y2H) assays

The yeast two-hybrid assays were performed using the procedures as described previously [31]. Briefly, the full-length human NONO cDNA was cloned into pGADT7 plasmid and transformed into a Y187 yeast strain, while the full-length Huma PIN1 cDNA, the WW domain (amino acid, 1-138) of PIN1, or the PPIase domains (amino acid, 118-492) segments were cloned into pGBKT7 plasmids and transformed into Y2H Gold yeast strain. The yeast strains containing the desired plasmids were mated together to produce diploid cells. The diploid cells were first selected on synthetically defined (SD) media dropped out for leucine and tryptophan (SD/-Leu/-Trp) followed by selection on quadra-dropout media with the

restrictiveness of Leucine (L), Tryptophan (W), Histidine (H), and Adenine (A) (SD/-Leu/-Trp/-His/-Ade) for positive interaction.

Generation of silent mutations and rescue of the knockdown effect

The three silent mutations were introduced into the siRNA target region of wild-type human NONO expression plasmid using the procedure described previously [31]. Briefly, the full-length NONO cDNA was cloned into pCDNA3.1 (+) plasmid (Invitrogen), followed by the insertion of three silent mutations into the siRNA targeted region (Δ3) of wild-type NONO expression plasmid to rescue the siRNA-induced phenotype. Silent mutations were verified by DNA sequencing analysis.

NONO

Wt : G GCC AGC AGC CAA AAT GAA GGC TTG ACT AT**T** GA**C C**TG AAG AAT TTT AGA AAA C

Δ3: G GCC AGC AGC CAA AAT GAA GGC TTG ACT AT**A** GA**T T**TG AAG AAT TTT AGA AAA C

A S S Q N E G L T I D L K N F R K

The MDA-MB-231 cells were transfected with siRNA for the knockdown-rescue experiment. The siRNA resistant NONO overexpression plasmid was transfected using Lipofectamine LTX ((ThermoFisher Scientific, Inc.) after 24 hours of siRNA transfection, as directed by the manufacturer. The serum-free media was replaced with full media 6 hours after transfection, and the cells were cultured for 48 hours to assess the NONO knockdown rescue using western blotting.

FRET imaging

To determine the interaction of PIN1 or PIN1-WW domain with NONO, FRET analysis was performed. First, the NONO sequence was amplified using Q5 polymerase (NEB) from pCDNA 3.1(+)-NONO (containing the full-length human NONO sequence, codon 1 to 471) and fused into a mVenus-C1 plasmid (#27794 Addgene) using Infusion HD cloning kit, the same procedures were performed for cloning the full-length human PIN1 sequence (codon 1 to 163) or PIN1-WW domain (codon 1 to 46) and PIN1-PPIase domain (codon 40 to 163) into the pmTurquoise-C1 (#60558 Addgene). The constructs prepared were verified by Sanger sequencing.

FRET experiments were performed using PFA-fixed HEK293T cells mounted onto a 24 well plate 20 mm round coverslips, transfected with dual expression plasmids: (i) mVenusC1-NONO and pmTurquoiseC1-PIN1, (ii) mVenusC1-NONO and pmTurquoiseC1-PIN1-WW domain, (iii) mVenusC1-NONO and pmTurquoiseC1-PIN1-PPIase domain, (iv) two plasmids mVenusC1/pmTurquoiseC1 expressing unfused mVenus (yellow) and Turquoise (cyan) proteins. Initially, fluorescence intensities of mVenus and mTurquoise were observed. The region of interest (ROIs) was then determined, and the acceptor photobleaching FRET assay between the fluorophores (mTurquoise and mVenus) was performed using laser scanning NIKON inverted confocal microscopy with *NIS* Elements software, objective lens and filters

for CFP (excitation 405 nm and emission 477nm/ 27nm bandwidth) and YFP (excitation 515nm and emission 527/48nm bandwidth). For acceptor photobleaching FRET assay the images are first captured with both CFP and YFP channels. The YFP partner is then photobleached using high intensity laser at 514 nm for 20s, after which the images were re-acquired with both CFP and YFP channels. The FRET energy transfer efficiency (E) was calculated from the equation: $E = 1- F_{pre}/F_{post}$ where F_{pre} and F_{post} are the donor fluorescence intensities within ROI before and after bleaching, respectively.

Immunoprecipitation

Magnetic dynabeads protein G (ThermoFisher Scientific) were washed and blocked with PBS supplemented with 5% BSA. The beads were resuspended in 200 µl PBS/BSA, and relevant antibodies (mouse IgG control and anti-NONO) were added, followed by rotation at room temperature for 2 hours. The bead-antibody complex was washed three times with PBS/BSA solution using the magnetic tube holder, and the supernatant was removed. Cells were lysed with non-denaturing lysis buffer (50 mM HEPES, 150 mM NaCl, 1% NP-40, 2 mM EDTA, 0.2 mM PMSF, 1 mM DTT, 5% glycerol) at 4 ˚C for 10 minutes with gentle rolling. Cells were sonicated 3 times for 5-second pulse each and centrifuged at 10000 g for 20 minutes at 4˚C. The concentration of protein was determined using a BCA kit (ThermoFisher Scientific). 40µl of lysate was collected for input, and 700 ug (300 µl) lysate was added to the bead-IgG and bead-primary antibody complex and incubated overnight at 4 ˚C with gentle rotation. On the next day, the bead-antibody with precipitated protein was washed 5 times with lysis buffer with one-minute rotation at 4˚C for each wash. The bead-antibody complexes were resuspended in 2XSDS lysis buffer and boiled at 100˚C for 5 minutes, along with the input. The supernatant was transferred into fresh tubes for immunoblotting analysis using a magnetic separation rack.

Immunohistochemistry (IHC) analysis

After deparaffinization, hydration, and washing, the tissue sections were immersed in Tris-EDTA buffer (pH 9) at boiling temperature for 15 minutes for antigen retrieval. The slides were immersed in 3%H2O2 for 20 minutes to block endogenous peroxidase reaction. The slides were washed with TBST buffer and blocked with 3% BSA for 20 minutes and then incubated with anti-NONO and anti-PIN1 primary antibodies diluted in blocking buffer at 4˚C overnight. According to the manufacturer's instructions, the slides were processed using EnVision+ Dual Link System-HRP kit (DAKO) and counterstained using hematoxylin. All IHC data were evaluated and scored from 1 to 3 based on the intensity of expression. The quick score method was used to perform pathological scoring [34]. The score of expression intensity was multiplied by the percentage of stained cells (denoted as 3 if the percentage of stained cell > 50%, 2 if the percentage of the stained cell is 25-50 %, and 1 if the percentage of the stained cell is < 25%) and defined as high or low expression.

Immunoflourecence (IF) analysis

Cells were seeded on the coverslips at an appropriate 60% confluence. After 24 hours of seeding the cells were transfected with siRNA-scr or siRNA-NONO. At 72 hours post transfection the cells were fixed by 4%

PFA for 10 minutes at room temperature, and washed three times with ice cold PBS for 5 minutes each. Cells were permeabilized with 0.2% Triton X-100 and blocked in 1% BSA, 22.52 mg/ml glycine in PBST for 1 hour at RT and incubated in the diluted antibody in 1% BSA in PBST (1: 100) in a humidified chamber overnight at 4 ˚C. Cells were then incubated in Goat anti-Mouse IgG-FITC secondary antibody solution (Thermo, 1:250 in PBST) for 30 minutes at room and counterstained with 1 µg/ml DAPI for 1 minutes. Subsequently, fluorescence was observed under Nikon Eclipse Ti microscope.

Bioinformatic analysis

OMICS data of breast tumors and normal tissues were analyzed using the Tumor Immune Estimation Resource TIMER (https://cistrome.shinyapps.io/timer/), UALCAN (http://ualcan.path.uab.edu/), and TNMplot (https://tnmplot.com/) web tools.

Statistical analysis

Statistical analysis was performed using GraphPad Prism (GraphPad Software, San Diego, CA, USA) and Microsoft Excel; data were presented as mean ± SD. The unpaired two-tailed t-test or ANOVA test was used to compare various groups. The correlation between PIN1 and NONO was determined using Spearman's rank correlation. The Mann-Whitney test was used to compare quick scores between paired breast cancer and adjacent tissues, and for the tracking measurements. A *p*-value of less than 0.05 was considered statistically significant.

Results

Breast cancers have the elevated expression of NONO.

To investigate the differential expression of NONO between tumor and normal tissues, the TCGA data expression analysis was performed using the TIMER web tool. It was found that NONO expression is significantly upregulated in multiple cancers, including breast cancer (Fig. 1a). Consistently, the data retrieved from TCGA using UALCAN showed higher mRNA expression in breast cancer tissues than in normal breast tissues (Fig. 1b). Mining of gene chip data from Gene Expression Omnibus (GEO) or RNA-seq data from TCGA, Therapeutically Applicable Research to Generate Effective Treatments (TARGET), and the Genotype-Tissue Expression (GTEx) databases using TNMplot demonstrated a significant upregulation of NONO in primary and metastatic carcinoma than in normal tissue (Fig. 1c).

To confirm the increased expression of NONO in breast cancer tissue as compared to adjacent normal tissue by immunohistochemistry (IHC), we validated the specificity of antibodies used for IHC analysis by siRNAs knockdown strategy. Protein lysates from NONO and PIN1 knockdown MDA-MB-231 cells were used to authenticate antibody specificity by immunoblot analysis. A single band of appropriate size was observed for NONO (~ 54 kDa) and PIN1 (~ 18 kDa) . The signals disappeared for target proteins in NONO and PIN1 knockdown cells using anti-NONO and anti-PIN1 mouse monoclonal antibodies, respectively (Supplementary Fig S1A, B) that confirms the specificity of anti-NONO and anti-PIN1

antibodies. The specificity of antibodies was further validated using immunofluorescence microscopy (Supplementary Fig. S1C, D). Immunohistochemical analysis of NONO protein expression further confirmed a significant increase in the expression of NONO in breast cancer tissues compared to their adjacent normal tissues (Fig. 1d, e). These results indicated that NONO expression is upregulated in breast cancer and could play an important role in breast cancer progression.

Next, the expression of NONO among patients based on different clinical parameters was investigated using the UALCAN online database. Based on individual cancer stages, statistical analysis indicated a significant increase in NONO expression in stage 1 2, 3, and 4 of breast cancer tissues compared to normal (Fig. 1f). In addition, TCGA data from UALCAN further revealed a significantly increased expression of NONO in different subclasses (Luminal, HER2 positive, and TNBC) of breast cancer tissue compared to normal tissues (Fig. 1g). Moreover, datasets retrieved from Clinical Proteomic Tumor Analysis Consortium (CPTAC) using the UALCANS tool revealed a higher expression of NONO protein in breast cancer tissues, as well as in different stages and subtypes of breast cancer as compared to normal (supplementary Fig. S2 A-C) demonstrating concordance with TCGA datasets. These results indicate that NONO expression and tumor progression are closely correlated.

NONO interacts specifically with PIN1, and this interaction is dependent on the N-terminal (WW) domain of PIN1.

In the previous work [28], NONO is ranked among the top proteins with functions similar to peptidylprolyl cis/trans isomerase (PIN1). PIN1 is an oncoprotein commonly implicated in cancers, and the function of PIN1 is defined by its two domains: WW domain and PPIase domain. It has been demonstrated that the WW domain has a stronger affinity for its substrate than the PPIase domain [35] and the binding of the WW domain with the substrate enables PIN1 to perform molecular function via the PPIase domain [36]. Earlier, the interaction between PIN and NONO was revealed *in vitro* [37]. Using an independent yeast-two-hybrid assay, we confirmed the interaction between human NONO and PIN1 and identified the functional WW domain (1-138 amino acids) of PIN1 essential for direct interaction with NONO (Fig. 2a).

The interaction of NONO with PIN1 and the WW domain of PIN1 was further confirmed using the acceptor photobleaching FRET technique. During acceptor photobleaching, the intensities of CFP (FRET donor: cyan fluorescence protein) and and YFP (FRET acceptor: yellow fluorescence protein) were monitored, and the images were taken before and after photobleaching of YFP within a region of interest (ROI). It was observed that for the FRET pair NONO-YFP/PIN1-CFP, and NONO-YFP/ PIN1-WW-CFP, the CFP intensities increased after acceptor photobleaching at several time points while no increase in the intensity of CFP was observed in NONO-YFP/PIN1-PPIase pair (Fig. 2b, Supplementary Fig. S3A-C). As shown in Fig. 2c the average FRET efficiency was 7.72 % and 12.63 % upon bleaching (post-bleach) in PIN1-CFP/NONO-YFP and PIN1-WW-CFP/NONO-YFP samples, respectively, as compared to control (samples with empty CFP and YFP vectors). As expected, FRET efficiency of samples co-transfected with PIN1-PPIase-CFP/NONO-YFP showed no increase in CFP fluorescence intensity, which further validates that WW domain but not the PPIase domain of PIN1 is essential for the direct interaction with NONO.

Since human NONO ORF (CCDS14410.1) has four threonine-proline (thr-pro) sites (Fig. 2d), we sought to identify the thr-pro binding site(s) critical for interaction with the PIN1-WW domain. Four threonine residues at positions 15, 410, 428, and 450 of NONO were substituted with glycine individually, and the yeast-two hybrid was performed. Our results demonstrated that a single mutation did not abolish the interaction of NONO with the PIN1-WW domain. However, reduced growth in response to protein-protein interaction was observed in yeast diploids containing substitution mutation T428A, demonstrating a moderate affinity of Thr_{428}-Pro_{429} for the WW domain of PIN1. Next, substituting threonine residues with glycine in all the four thr-pro sites resulted in the complete abrogation of NONO interaction with the PIN1-WW domain. Further, we analysed thr-pro motifs important for the interaction of NONO with the PIN1-WW domain. No interaction was observed between NONO containing T410A, T428A, and T450A mutations and the PIN1-WW domain. Substitution mutations T410A and T15A generated the mutant NONO protein still able to interact with the PIN1-WW domain. However, the substitution of T428A and T450A completely abrogates the interaction of NONO with the PIN1-WW domain, indicating that two thr-pro binding sites at the C-terminal side are essential for the interaction of NONO with the WW domain of PIN1 (Fig. 2e).

The stability of NONO is regulated by PIN1.

To determine the effect of PIN1 inhibition on NONO, we used the PIN1 inhibitor Juglone [38]. Because NONO binds to PIN1 directly, we then asked whether the protein-protein interaction between NONO and PIN1 promotes NONO stability. For this, we treated the MDA-MB-231 cells with Juglone and examined the effect of proteasome inhibitor MG-132 in Juglone-treated cells. Our results revealed that Juglone increased the loss of NONO protein, and the treatment of MG132 completed blocked the Juglone-induced loss of NONO (Fig. 3a), indicating that PIN1 promotes stability of NONO by preventing the proteasomal degradation.

Since the expression of NONO protein was upregulated in human breast cancer tissues, PIN1 binding to NONO enhances its stability. Next, we performed the IHC to examine the expression of PIN1 protein in the same groups of human breast cancer sections. We observed a significant increase in the expression of PIN1 protein in breast cancer tissues (14 out of 20, 70%) compared to normal adjacent tissues (Fig. 3b, c). Statistical analyses further revealed a significant correlation (Spearman's Rank Correlation (r_s) = 0.4645, P = 0.01) between PIN1 and NONO (Fig. 3d) in human breast cancer tissues, indicating that binding of PIN1 to NONO is involved in the oncogenic behavior of breast cancer cells.

The silencing of NONO gene expression decreases the cell viability and colony-forming ability of breast cancer cells.

To gain essential insight into the function of the NONO gene, we first evaluated the knockdown efficiency of siRNA-NONO at the transcription level of the target gene and the corresponding protein level using RT-PCR and western blotting, respectively. It was demonstrated that siRNA-NONO efficiently reduced the mRNA and protein levels of the NONO gene in both MDA-MB-231 and MCF-7 cells (Fig. 4a, b). Next, the rescue experiment was performed to determine the specificity of siRNA, NONO human cDNA was cloned

into pcDNA3.1(+), and the three silent mutations were introduced into NONO ORF to make the construct resistant to siRNA, and the silent substitution mutations were confirmed in their entirety using Sanger sequencing (supplementary Fig. S4a, b). Transfection of exogenous mutant NONO constructs rescued the expression of NONO and PCNA when cotransfected with the corresponding siRNA-NONO (Supplementary Fig. S4c), indicating that the siRNA is highly selective and specific for the endogenous NONO gene. In addition, the expression profile of NONO protein was observed in different breast cancer cells. Western blot analysis revealed that compared with the normal human mammary epithelial cells (MCF10A), the expression of NONO was particularly overexpressed in the human breast cancer cell lines MCF-7, MDA-MB-231, T47D and MDA-MB-453. The result suggests that NONO has a critical role in the development of human breast cancers (Supplementary Fig. S5).

To explore whether silencing of NONO gene expression affects the oncogenic behaviour of breast cancer cells, the crystal violet and colony formation assays were performed. Crystal violet assay revealed a significant decrease in the viability of siRNA-NONO transfected MDA-MB-231 and MCF-7 cells compared to siRNA-scr after 72 hours of transfection (Fig. 4c). Next, we examined the colony-forming ability of NONO silenced breast cancer cells. Compared to siRNA-scr transfected breast cancer cells, NONO knockdown MDA-MB-231 and MCF-7 showed the reduced colony-forming ability as demonstrated by colony-forming assay (Fig. 4d). These results suggest the involvement of NONO in regulating the tumorigenic properties of breast cancer cells.

Silencing of NONO induces the S-phase cell cycle arrest in breast cancer cells.

To investigate the effect of NONO knockdown on cell cycle progression, flow cytometry was used to analyse the phase distribution of cell cycle in siRNA transfected breast cancer cells. Compared to siRNA-scr transfected cells, the knockdown of NONO in MDA-MB-231 and MCF-7 cells significantly arrests the cell at the S-phase of the cycle, with a concomitant decrease in the percentage of cells in the G2/M phase in the case of MDA-MB-231 and, G0/G1 and G2/M phase in MCF-7 cells (Fig. 5a).

In accordance with the cell-cycle distribution analysis, we examined the effect of the silencing of NONO on the expression of markers related to the cell cycle. Real-time PCR analysis demonstrated that silencing of NONO significantly elevated the mRNA expression levels of cyclin E and CDKN1A (p21) (Fig. 5b). p21 has the unique ability to inhibit cyclin-dependent kinase blocks PCNA dependent DNA replication and causes the arrest in the S phase of the cell cycle [39]. Our results showed that at the protein level, the expression of PCNA was decreased in both MDA-MB-231 and MCF-7 NONO knockdown cells (Fig. 5c). Taken together, the above results suggest that the accumulation of NONO silenced cells in the S phase can be due to the induction of p21 and the inhibition of PCNA.

Silencing of NONO induces apoptosis and promotes changes in mitochondrial membrane potential.

To analyze the impact of silencing of NONO on cell death by apoptosis, a flow cytometry analysis using annexin-V/propidium-iodide assay was performed. In both MDA-MB-231 and MCF-7 cells line, a significant increase in the apoptotic index was observed in breast cancer cells with the knockdown of

NONO compared to siRNA-scr transfected cells (Fig. 6a). After 72 hours of transfection, a fraction of apoptotic cells reached 22.61 ± 1.8 percent and 46.1 ± 1.19 percent in MDA-MB-231 and MCF-7 cells, respectively, compared to control with 7.49 ± 1.9 percent in MDA-MB-231 and 26.8 ± 1.4 percent in MCF-7 cell. Furthermore, we investigated the effect of NONO knockdown on the expression of apoptosis-regulating molecules; western blotting analysis revealed that NONO gene silencing effectively increased the level of pro-apoptotic Bax in MDA-MB-231 and MCF-7 cells as well as cleaved caspase 3 in MCF-7 cells while reducing the levels of anti-apoptotic Bcl-2 proteins in both MDA-MB-231 and MCF-7 cell after 72 hours of transfection (Fig. 6b, c). Next, we determined the effect of the silencing of NONO on the expression of p53 in MCF-7 cells. It was observed that the silencing of NONO increased the expression of p53 and p-p53 proteins. Further, treatment of MCF-7 cells with p53 inhibitor pifithrin-α does not affect NONO expression. In contrast, the treatment of MCF-7 cells with H_2O_2 at a 50 μM concentration for 6 hours induces the expression of NONO (Fig. 6d). This indicates that NONO can be a new drug target for selectively promoting p53 mediated cell cycle arrest and apoptosis in breast cancers with wild-type p53.

Further, we used flow cytometry to investigate the effect of NONO depletion on the change of mitochondrial membrane potential of MDA-MB-231 and MCF-7 cells using JC-1 dye. It was demonstrated that silencing of NONO in MDA-MB-231 and MCF-7 caused a reduction in mitochondrial membrane potential compared to scramble, as seen by a rise in the green-to-red (monomer/aggregate) ratio. Following the knockdown of NONO in MDA-MB-231, the JC-1 green/red ratio was significantly increased to 0.344 ± 0.01 from 0.07 ± 0.05 in a scrambled group. Similarly, on knockdown of NONO in MCF-7 cells, the JC-1 green/red ratio was increased to 0.20 ± 0.02 from 0.03 ± 0.01 in the scrambled group. These results suggest that silencing NONO causes mitochondrial dysfunction via modifying the mitochondrial membrane potential (MMP) (Fig. 6e). Since loss of mitochondrial membrane potential (ΔΨm) during the redox stress is associated with ROS-induced apoptosis. We investigated the effect of silencing of NONO on ROS generation using MitoSOX red fluorescent dye by flow cytometry. It was observed that depletion of NONO significantly increased the ROS strength in MDA-MB-231 cells compared to scramble (Supplementary Fig. S6), indicating NONO prevents apoptosis by inhibiting ROS generation.

Silencing of NONO reduces the migratory and invasive potentials of breast cancer cells.

To demonstrate the effect of silencing of NONO on the migratory potential of breast cancer cells. First, the wound healing assay was performed. As shown in Fig. 7a, b; depletion of NONO in MDA-MB-231 and MCF-7 resulted in reduced recovery of artificial wound area compared to siRNA-scr transfected cells when examined at the same time point after 12, 24, and 48 hours.

Next, transwell inserts coated with/without matrigel were used to investigate the invasive and migratory potential of siRNA NONO knockdown MDA-MB-231 and MCF-7 cells. It was found that NONO knockdown significantly reduced the ability of breast cancer cells to migrate and invade (Fig. 7c). Furthermore, western blot analysis was performed to examine the expression levels of migration-related proteins. It was revealed that silencing of NONO alters the protein expression levels of matrix metalloproteinases (MMPs) and epithelial-mesenchymal transition (EMT)-related molecules in breast cancer cells. The

expression of MMP-2, and MMP-9 was inhibited, while the expression of epithelial marker protein E-cadherin was increased, and the expression of mesenchymal marker vimentin was decreased upon the silencing of the NONO gene (Fig. 7d). Next, MDA-MB-231 cells with known invasion/metastatic capabilities were investigated whether high NONO expression would cause MDA-MB-231 breast cancer cells to disseminate throughout zebrafish using the described experimental settings[40][41]. Green CMFDA stained scrambled and NONO siRNA transfected cells were injected into perivitelline space of 48 hours post-fertilization (hpf) zebrafish embryos and examined at 72 hours post-injection (hpi). Quantitative analysis of fluorescent tumor cells per zebrafish embryo using modified version of Fiji software demonstrated that silencing of NONO significantly decreased the number of migrated cells in zebra fish embryos when compared to control group (Fig. 7e). This data is consistent when we performed an independent experiment (Supplementary Fig. S7), thereby supporting the role of NONO in the proliferation and metastasis of breast cancer cells in the zebrafish xenograft model. Collectively, these results suggest that NONO is a positive regulator in cell migration and invasion and induces the EMT of breast cancer cells.

NONO promotes the population of cancer stem cells (CSCs) in breast cancer.

Cancer stem cells have been demonstrated to promote tumor initiation and development, metastasis, relapse and resistance to treatment. To determine the role of NONO in the stemness of breast cancer cells, we generated NONO knockout MDA-MB-231 and MCF-cells using the CRISPR-Cas9 system. The successful knockout of the *NONO* gene in MDA-MB-231 and MCF-7 cell lines was confirmed by western blotting (Supplementary Fig. S8). Breast cancer cells that express the phenotypic $CD24^{\blacksquare}/CD44$ markers on their surface have stem cell-like characteristics, including the ability to self-renew and initiate tumours [42]. Flow cytometry analysis revealed that knockout of *NONO* gene significantly reduced the population of $CD24^{\blacksquare}/CD44$ cells in MDA-MB-231 and MCF-7 cells (Fig. 8a). Additionally, silencing of NONO reduced the mRNA levels of several core pluripotency stem cell regulators (*OCT4, SOX2, Slug,* and *Twist*) in MDA-MB-231 and MCF-7 cells (Fig. 8b, c). Since the PIN1 is highly expressed in most cancers, especially in cancer stem cells [40, 41]. We investigated the effect of the silencing of NONO on the expression of PIN1. RT-qPCR and western blot analysis revealed that silencing of NONO significantly reduced the mRNA and protein levels of PIN1, indicating that NONO promotes CSC-like properties in breast cancer cells via the regulation of PIN1 (Fig. 8d - f).

Silencing of NONO increases PD-L1 expression at the surface of breast cancer cells.

Programmed cell death protein 1 ligand (PD-L1) is an inhibitory molecule expressed by tumor cells to induce anergy on tumor-reactive cells [45], [46]. The increased expression of PD-L1 in cancer cells using multiple approaches augments immune checkpoint block therapy response in experimental models [47] [48]. To determine the effect of the silencing of NONO on the expression of PD-L1, a flow cytometry analysis was performed using an anti-PD-L1 APC antibody. It was demonstrated that silencing of NONO significantly increased the expression of PD-L1 both in MDA-MB-231 and MCF-7 cells (Fig. 9).

Silencing of NONO suppresses the activation of the Akt/MAPK/β-catenin signalling pathway.

To explore the relation between NONO and MAPK signalling pathway, western blotting assay was performed to detect the protein expression of PTEN, p-Akt, p-p38, p-Erk, eIF4E, NF-kB, p-NF-kB, and RACK-1. It was revealed that compared to siRNA-scr transfected breast cancer cells, the silencing of NONO promotes the protein expression of PTEN while reducing expression levels of p-Akt, p-Erk, p-P38, NF-kB, p-NF-kB, eIF4E, and RACK-1 both in MDA-MB-231 and MCF-7 cells (Fig. 10a). Moreover, we characterized the interaction of NONO with c-Jun using yeast two-hybrid system (Fig. 10b). The interaction was further validated by NONO immunoprecipitation/western blot analysis using MCF-7 lysate (Fig. c). In addition, a physical interaction was also observed between endogenous NONO and β-catenin proteins in MCF-7 cells using IP/Western blotting analysis (Fig. 10d), suggesting that NONO forming a complex with β-catenin might be involved in the tumor progression of breast cancer cells by affecting the β-catenin pathway. Since β-catenin signalling is considered to be a major regulator of cancer stem-cell (CSC) self-renewal. We hypothesized that silencing of NONO may inactivate β-catenin signalling and thus inhibit the stem cell-like properties and tumorigenicity in breast cancer cells. To test this hypothesis, we examined that the silencing of NONO inhibits the expression of β-catenin. Consistently, the expression of well-known downstream targets of β-catenin, such as c-myc, and CCND1 have consistently downregulated in NONO silenced MDA-MB-231 and MCF-7 cells (Fig. 10e). Taken together these results suggest that NONO promotes the tumorigenicity of breast cancer cells via the activation of the Akt/MAPK/β-catenin pathway.

Discussion

NONO has been found to promote the development of breast cancer [12], prostate cancer [17], and hepatic [49] cancer. In this study, we have identified PIN1 as a positive regulator of NONO and contributes to the tumor promoting activity of NONO. Inhibition of PIN1 reduced the levels of NONO protein in MDA-MB-231 breast cancer cells. While PIN1 binds to c-terminal thr-pro motifs of NONO and regulates its stability in breast cancer, it is likely that in breast cancer cells the overexpression of PIN1 contributes to more stable and abundant NONO that promotes tumorigenesis by activating cancer-promoting genes and inactivating tumor suppressors.

We examined the expression of NONO in breast cancers using database mining, reported the higher expression of NONO in breast cancer tissues. We investigated the effect of silencing of NONO on viability, cell proliferation, cell cycle, migration and invasion, apoptosis and stemness of breast cancer cells *in vitro,* and the effect of NONO knockdown on the migration potential of human breast cancer cells in *in vivo* zebrafish xenograft model. In addition we have revealed novel interaction of NONO with c-Jun and β-catenin, and elucidated the critical role of NONO as a novel regulator Akt/MAPK/β-catenin signalling, indicating the contribution of NONO to breast cancer progression and demonstrated a basis for considering NONO as a breast cancer therapeutic candidate.

To better understand the role of NONO in the development of breast cancer, siRNA technology was used to knock down the NONO gene in MDA-MB-231 and MCF-7 breast cancer cell lines. One of the most

significant drawbacks of using siRNAs in experimentation is the likelihood of off-target effects. Ectopic expression of siRNA resistant construct is considered a gold standard stringent approach to confirm the specificity of siRNA[50][51]. Hence to confirm the specificity of siRNA used in the study, we performed the rescue experiment, employing the expression construct containing three silent point mutations within the respective regions targeted by siRNA. Following the transfection of siRNAs, NONO expression was significantly downregulated at both the mRNA and protein levels, as confirmed by qRT-PCR and western blot in both MDA-MB-231 and MCF-7 cells lines.

Modulation of the cell cycle is frequently linked to changes in cell proliferation [52]. In this study, we observed a significant increase in S phases MDA-MB-231 and MCF-7 cells after transfection with siRNA-NONO as compared to cells transfected with siRNA-scr. These results suggest that NONO plays an essential role in cell cycle progression, and the anti-proliferative effect of NONO knockdown in breast cancer cells was most likely due to arrest in the S phase. We hypothesized that NONO silencing would alter the expression of cell cycle-related genes. We investigated by qRT-PCR analysis that p21 (CDKN1A), a major regulator of S-phase progression, was highly expressed in NONO knockdown cells. p21 has a peculiar ability to interact with PCNA and inhibits its activity[39]. p21 negatively regulates DNA replication by binding the proliferating cell nuclear antigen (PCNA) and altering its interaction with alternative DNA polymerases, in addition to its role as a CDK inhibitor [38, 50]. PCNA deficiency blocks DNA synthesis and causes cells to enter the S phase of the cell cycle [54]. Cyclin D is highly expressed in the mid-to-late G1 phase and exhibits an up-regulated kinase activity when bound to cdk4 (predominantly cyclin D1/cdk4 complex) in cancer cells [55]. The maximal level of cyclin D during the G1 phase is required for the cell to initiate DNA synthesis but must be repressed at a low level during the S phase for effective DNA synthesis [56]. It was demonstrated that silencing of NONO resulted in a marked decrease of cyclin D1 after 72 hours of transfection both in MDA-MB-231 and MCF-7 cells, which indicates an arrest in the S-phase cell cycle. The growth suppressor p53 is a tightly controlled transcription factor that, depending on its expression levels, can cause cell cycle arrest or apoptosis [57]. We analyzed the expression level of p53, a potent inducer of p21, in MCF-7 and found that silencing of NONO promotes the up-regulation of p53 and p-p53 proteins. Since the p53 is functional in MCF-7 cells but mutated in MDA-MB-231. Based on this finding, we can suggest that silencing of NONO induces S-phase arrest independent of p53, and the arrest might be mainly due to p21 overexpression. In breast cancers with functional p53, targeting NONO can be a novel strategy for promoting p53 mediated cell cycle arrest and apoptosis.

Tumor cells can develop the ability to migrate and invade beyond their normal boundaries and seed new tumors at distant sites [58]. Silencing of NONO gene expression in MDA-MB-231 and MCF-7 reduced the migratory and invasive capabilities compared to control. Additionally, we found that NONO knockdown cells had elevated E-cadherin and reduced MMP-2, MMP-9, and vimentin protein levels, indicating that NONO regulates the metastatic processes in breast cancer via modulating the migration related proteins. In high-grade tumors, MMPs are overexpressed and secreted extracellularly in the form of zymogens. Activated MMPs destroy the extracellular matrixes, thereby causing the loss of cell-cell adhesion, subsequently migration and invasion of cancer cells in solid tumors [59]. MMP-2 and MMP-9 have been directly linked to the metastatic process of breast cancer [60]. The inhibition of the protein levels of MMP-

2 and MMP-9 in NONO silenced breast cancer indicates that NONO regulates the migratory and invasive capabilities of breast cancer cells. To test whether silencing of NONO can inhibit the migration potential of breast cancer cells *in vivo*, we harnessed xenotransplantation zebrafish embryo model, which has evolved as a powerful model for studying metastasis. Knockdown of NONO in MDA-MB-231 cells led to loss of proliferation and metastasis capacities at the new locations.

In addition, we examined the expression of E-cadherin and vimentin. Vimentin is a type III intermediate filament protein that plays an important role in breast cancer cell migration and invasion and promotes the epithelial-mesenchymal transition [61][62]. The migration of cancer cells and E-cadherin levels are inversely correlated [63]. The loss of the intercellular adhesion protein E-cadherin is thought to trigger invasion to adjacent tissues and metastasis [64]. Our study demonstrated that silencing of NONO reduced the vimentin and elevated the E-cadherin protein levels thereby inhibiting the metastasis and EMT of breast cancer cells.

Studies have revealed that cancer cells that have presumably undergone EMT may also have a CSC phenotype. CSCs, a small number of self-renewing cells found inside tumors, have been shown to drive tumor development, relapse, and distant metastasis, according to extensive studies conducted over many years [42][65]. Since $CD24^{-}/CD44^{+}$ phenotype is commonly used to characterize CSCs [42], our results suggest that knockout of NONO significantly reduced the $CD24^{-}/CD44^{+}$, revealing that NONO is a positive regulator of breast cancer stem cell-like properties. Most cancers have a high level of PIN1 expression that induces stem cell-like traits. We demonstrated that the silencing of NONO inhibits the PIN1 expression thereby inhibiting the CSC formation in breast cancer. The underlying mechanism of how NONO promotes the tumorigenicity of breast cancer cell survival, proliferation, migration, invasion, and stemness remains unknown. The MAPK and β-catenin pathways have been reported to be involved in breast cancer cell survival, proliferation, migration and invasion, and stemness. We have investigated that silencing of NONO altered p-Erk, p-Akt, p-P38, eIF4E, RACK-1, and PTEN levels, indicating that NONO directly affects the Akt/MAPK signalling pathway that regulates cell proliferation, and migration and invasion of breast cancer cells. Since β-catenin signalling is considered a critical regulator of stemness of breast cancer cells, our results demonstrated that knockdown of NONO reduced the β-catenin protein level. Consistently, the downstream targets of Wnt/β-catenin: c-myc, CCND1, CD44 were also down-regulated. Further, Immunoprecipitation analysis has revealed the NONO as a β-catenin and c-Jun interacting partner, indicating the direct involvement of NONO in β-catenin and MAPK pathways. In addition, we demonstrated that silencing of NONO promotes the expression of PD-L1 at the surface of breast cancer cells, which is consistent with the recent finding that inhibition of PIN1 elevated the expression of PD-L1[48] in human cancers that could potentiate immune checkpoint blockade.

In conclusion, this study provides insights that NONO functions as oncogene to promote breast tumorigenicity by regulating the expression/activation of genes involved in cell proliferation, cell survival, migration and invasion, EMT and stem cell formation, as well as by activating Akt/MAPK/β-catenin signalling pathways. These are the critical processes in cancer progression, thus targeting NONO in

breast cancer could be a novel therapeutic approach, and could show better antitumor efficiency in combination with immunotherapy.

Declarations

Acknowledgments

The authors thank Abu Rayhan, Abhishek Rohilla, Abarna Krishnakumar, Tariq Pacha Khan, and Shirani Punniyamoorthi for their technical assistance. Nitin Sharma is thanked for help in confocal microscopy experiments. National Institute of Pathology, Safdarjung Hospital Campus for providing facilities for Immunohistochemistry experiments. S.V was supported by University Grants Commission (UGC) research fellowship for doctoral programme.

Funding

This research project was partially supported by the Indian Council of Medical Research (ICMR) Project No. 2020-4505/CMB/ADHOC-BMS and Department of Science and Technology, New Delhi (Grant - GAP0245). The funders had no role in study design, data collection and analysis, decision to publish or preparation of article.

Authors Information

Affiliations:

Cancer Biology Laboratory, Faculty of Life Science and Biotechnology, South Asian University, Akbar Bhawan, Chanakyapuri, New Delhi-110021, India

Bilal Ahmad Lone, Preeti Nagar, Faiz Ahmad, and Yuba Raj Pokharel

National Institute of Pathology, Safdarjung Hospital Campus, Room No.610, 6th Floor, Ansari Nagar, New Delhi, 110029, India

Fouzia Siraj, and Ira Sharma

CSIR-Institute of Genomics and Integrative Biology (CSIR-IGIB), New Delhi-110025, India

Shweta Verma and Chetana Sachidanandan

Academy of Scientific and Innovative Research (AcSIR), Gaziabad- 201002, India

Shweta Verma and Chetana Sachidanandan

Corresponding author: Yuba Raj Pokharel, yrp@sau.ac.in

Contributions: Y.R.P and B.A.L conceived the study and designed the experiments. B.A.L., F.S., P.N, I.S. S.V, S.K.L.K, and F.A., performed the experiments. C.S provided the input and research facility for zebrafish experiments. B.A.L and Y.R.P wrote the manuscript and analyzed the data.

Ethics approval and consent to participate: National Institute of Pathology, Safdarjung hospital, Ansari Nagar, New Delhi, 110029, India, have generously provided IHC data with their institutional ethical committee approval. The animal study was carried out in accordance with the guidelines of laboratory animal care and the experimentation protocols has been approved by the CSIR-IGIB Institutional Animal Ethics Committee (IAEC).

Consent for publication: Availability of data and material: The datasets used and analyzed during the current study are available from the corresponding authors on reasonable request.

Ethics Declarations

Competing interests

Authors declare no competing interest.

References

1. H. Sung *et al.*, “Global Cancer Statistics 2020: GLOBOCAN Estimates of Incidence and Mortality Worldwide for 36 Cancers in 185 Countries.,” *CA Cancer J Clin*, vol. 71, no. 3, pp. 209–249, May 2021.
2. B. Weigelt, J. L. Peterse, and L. J. van ’t Veer, “Breast cancer metastasis: markers and models.,” *Nat Rev Cancer*, vol. 5, no. 8, pp. 591–602, Aug. 2005.
3. A. R. Safa, “Resistance to Cell Death and Its Modulation in Cancer Stem Cells.,” *Crit Rev Oncog*, vol. 21, no. 3–4, pp. 203–219, 2016.
4. M. Luo, M. Brooks, and M. S. Wicha, “Epithelial-mesenchymal plasticity of breast cancer stem cells: implications for metastasis and therapeutic resistance.,” *Curr Pharm Des*, vol. 21, no. 10, pp. 1301–1310, 2015.
5. B. Dong, D. S. Horowitz, R. Kobayashi, and A. R. Krainer, “Purification and cDNA cloning of HeLa cell p54nrb, a nuclear protein with two RNA recognition motifs and extensive homology to human splicing factor PSF and Drosophila NONA/BJ6.,” *Nucleic Acids Res*, vol. 21, no. 17, pp. 4085–4092, Aug. 1993.
6. P. Feng *et al.*, “NONO and tumorigenesis: More than splicing.,” *J Cell Mol Med*, vol. 24, no. 8, pp. 4368–4376, Apr. 2020.
7. C. M. Clemson *et al.*, “An architectural role for a nuclear noncoding RNA: NEAT1 RNA is essential for the structure of paraspeckles.,” *Mol Cell*, vol. 33, no. 6, pp. 717–726, Mar. 2009.
8. X. Dong, J. Sweet, J. R. G. Challis, T. Brown, and S. J. Lye, “Transcriptional activity of androgen receptor is modulated by two RNA splicing factors, PSF and p54nrb.,” *Mol Cell Biol*, vol. 27, no. 13,

pp. 4863–4875, Jul. 2007.

9. Y. Kanai, N. Dohmae, and N. Hirokawa, “Kinesin transports RNA: isolation and characterization of an RNA-transporting granule.,” *Neuron*, vol. 43, no. 4, pp. 513–525, Aug. 2004.
10. K. V Prasanth *et al.*, “Regulating gene expression through RNA nuclear retention.,” *Cell*, vol. 123, no. 2, pp. 249–263, Oct. 2005.
11. L. Jaafar, Z. Li, S. Li, and W. S. Dynan, “SFPQ•NONO and XLF function separately and together to promote DNA double-strand break repair via canonical nonhomologous end joining.,” *Nucleic Acids Res*, vol. 45, no. 4, pp. 1848–1859, Feb. 2017.
12. Z. Zhu *et al.*, “p54(nrb)/NONO regulates lipid metabolism and breast cancer growth through SREBP-1A.,” *Oncogene*, vol. 35, no. 11, pp. 1399–1410, Mar. 2016.
13. S.-J. Kim *et al.*, “RNA-binding protein NONO contributes to cancer cell growth and confers drug resistance as a theranostic target in TNBC.,” *Theranostics*, vol. 10, no. 18, pp. 7974–7992, 2020.
14. M. Shen *et al.*, “RNA-binding protein p54(nrb)/NONO potentiates nuclear EGFR-mediated tumorigenesis of triple-negative breast cancer.,” *Cell Death Dis*, vol. 13, no. 1, p. 42, Jan. 2022.
15. K. Iino *et al.*, “RNA-binding protein NONO promotes breast cancer proliferation by post-transcriptional regulation of SKP2 and E2F8.,” *Cancer Sci*, vol. 111, no. 1, pp. 148–159, Jan. 2020.
16. H. Ishiguro, H. Uemura, K. Fujinami, N. Ikeda, S. Ohta, and Y. Kubota, “55 kDa nuclear matrix protein (nmt55) mRNA is expressed in human prostate cancer tissue and is associated with the androgen receptor.,” *Int J cancer*, vol. 105, no. 1, pp. 26–32, May 2003.
17. R. Yamamoto *et al.*, “Overexpression of p54(nrb)/NONO induces differential EPHA6 splicing and contributes to castration-resistant prostate cancer growth.,” *Oncotarget*, vol. 9, no. 12, pp. 10510–10524, Feb. 2018.
18. S. Schiffner, N. Zimara, R. Schmid, and A.-K. Bosserhoff, “p54nrb is a new regulator of progression of malignant melanoma.,” *Carcinogenesis*, vol. 32, no. 8, pp. 1176–1182, Aug. 2011.
19. D. Li *et al.*, “Ets-1 promoter-associated noncoding RNA regulates the NONO/ERG/Ets-1 axis to drive gastric cancer progression.,” *Oncogene*, vol. 37, no. 35, pp. 4871–4886, Aug. 2018.
20. R. Cheng *et al.*, “Downregulation of NONO induces apoptosis, suppressing growth and invasion in esophageal squamous cell carcinoma.,” *Oncol Rep*, vol. 39, no. 6, pp. 2575–2583, Jun. 2018.
21. X. Z. Zhou and K. P. Lu, “The isomerase PIN1 controls numerous cancer-driving pathways and is a unique drug target.,” *Nat Rev Cancer*, vol. 16, no. 7, pp. 463–478, Jul. 2016.
22. E. S. Yeh and A. R. Means, “PIN1, the cell cycle and cancer.,” *Nature reviews. Cancer*, vol. 7, no. 5. England, pp. 381–388, May-2007.
23. Y.-C. Liou, X. Z. Zhou, and K. P. Lu, “Prolyl isomerase Pin1 as a molecular switch to determine the fate of phosphoproteins.,” *Trends Biochem Sci*, vol. 36, no. 10, pp. 501–514, Oct. 2011.
24. Q. Ding *et al.*, “Down-regulation of myeloid cell leukemia-1 through inhibiting Erk/Pin 1 pathway by sorafenib facilitates chemosensitization in breast cancer.,” *Cancer Res*, vol. 68, no. 15, pp. 6109–6117, Aug. 2008.

25. Z. Lu and T. Hunter, “Prolyl isomerase Pin1 in cancer.,” *Cell Res*, vol. 24, no. 9, pp. 1033–1049, Sep. 2014.
26. F. Suizu, A. Ryo, G. Wulf, J. Lim, and K. P. Lu, “Pin1 regulates centrosome duplication, and its overexpression induces centrosome amplification, chromosome instability, and oncogenesis.,” *Mol Cell Biol*, vol. 26, no. 4, pp. 1463–1479, Feb. 2006.
27. G. Wulf, P. Garg, Y.-C. Liou, D. Iglehart, and K. P. Lu, “Modeling breast cancer in vivo and ex vivo reveals an essential role of Pin1 in tumorigenesis.,” *EMBO J*, vol. 23, no. 16, pp. 3397–3407, Aug. 2004.
28. Y. R. Pokharel *et al.*, “Relevance Rank Platform (RRP) for Functional Filtering of High Content Protein-Protein Interaction Data.,” *Mol Cell Proteomics*, vol. 14, no. 12, pp. 3274–3283, Dec. 2015.
29. Y. Chen *et al.*, “Prolyl isomerase Pin1: a promoter of cancer and a target for therapy.,” *Cell Death Dis*, vol. 9, no. 9, p. 883, Aug. 2018.
30. Z. Asad *et al.*, “Rescue of neural crest-derived phenotypes in a zebrafish CHARGE model by Sox10 downregulation.,” *Hum Mol Genet*, vol. 25, no. 16, pp. 3539–3554, Aug. 2016.
31. B. A. Lone, F. Ahmad, S. K. L. Karna, and Y. R. Pokharel, “SUPT5H Post-Transcriptional Silencing Modulates PIN1 Expression, Inhibits Tumorigenicity, and Induces Apoptosis of Human Breast Cancer Cells.,” *Cell Physiol Biochem Int J Exp Cell Physiol Biochem Pharmacol*, vol. 54, no. 5, pp. 928–946, Sep. 2020.
32. B. A. Lone, S. K. L. Karna, F. Ahmad, N. Shahi, and Y. R. Pokharel, “CRISPR/Cas9 System: A Bacterial Tailor for Genomic Engineering.,” *Genet Res Int*, vol. 2018, p. 3797214, 2018.
33. N. E. Sanjana, O. Shalem, and F. Zhang, “Improved vectors and genome-wide libraries for CRISPR screening.,” *Nature methods*, vol. 11, no. 8. pp. 783–784, Aug-2014.
34. S. Detre, G. Saclani Jotti, and M. Dowsett, “A ‘quickscore’ method for immunohistochemical semiquantitation: validation for oestrogen receptor in breast carcinomas.,” *J Clin Pathol*, vol. 48, no. 9, pp. 876–878, Sep. 1995.
35. P. J. Lu, X. Z. Zhou, M. Shen, and K. P. Lu, “Function of WW domains as phosphoserine- or phosphothreonine-binding modules.,” *Science*, vol. 283, no. 5406, pp. 1325–1328, Feb. 1999.
36. C. Smet, J.-M. Wieruszeski, L. Buée, I. Landrieu, and G. Lippens, “Regulation of Pin1 peptidyl-prolyl cis/trans isomerase activity by its WW binding module on a multi-phosphorylated peptide of Tau protein.,” *FEBS Lett*, vol. 579, no. 19, pp. 4159–4164, Aug. 2005.
37. A. Proteau, S. Blier, A. L. Albert, S. B. Lavoie, A. M. Traish, and M. Vincent, “The multifunctional nuclear protein p54nrb is multiphosphorylated in mitosis and interacts with the mitotic regulator Pin1.,” *J Mol Biol*, vol. 346, no. 4, pp. 1163–1172, Mar. 2005.
38. M. R. Kim, H. S. Choi, J. W. Yang, B. C. Park, J.-A. Kim, and K. W. Kang, “Enhancement of vascular endothelial growth factor-mediated angiogenesis in tamoxifen-resistant breast cancer cells: role of Pin1 overexpression.,” *Mol Cancer Ther*, vol. 8, no. 8, pp. 2163–2171, Aug. 2009.
39. J. Chen *et al.*, “A 39 amino acid fragment of the cell cycle regulator p21 is sufficient to bind PCNA and partially inhibit DNA replication in vivo.,” *Nucleic Acids Res*, vol. 24, no. 9, pp. 1727–1733, May

1996.

40. I. Paatero, S. Alve, S. Gramolelli, J. Ivaska, and P. M. Ojala, “Zebrafish Embryo Xenograft and Metastasis Assay.,” *Bio-protocol*, vol. 8, no. 18, p. e3027, Sep. 2018.
41. Y. Teng, X. Xie, S. Walker, D. T. White, J. S. Mumm, and J. K. Cowell, “Evaluating human cancer cell metastasis in zebrafish.,” *BMC Cancer*, vol. 13, p. 453, Oct. 2013.
42. M. Al-Hajj, M. S. Wicha, A. Benito-Hernandez, S. J. Morrison, and M. F. Clarke, “Prospective identification of tumorigenic breast cancer cells.,” *Proc Natl Acad Sci U S A*, vol. 100, no. 7, pp. 3983–3988, Apr. 2003.
43. M.-L. Luo *et al.*, “Prolyl isomerase Pin1 acts downstream of miR200c to promote cancer stem-like cell traits in breast cancer.,” *Cancer Res*, vol. 74, no. 13, pp. 3603–3616, Jul. 2014.
44. A. Rustighi *et al.*, “Prolyl-isomerase Pin1 controls normal and cancer stem cells of the breast.,” *EMBO Mol Med*, vol. 6, no. 1, pp. 99–119, Jan. 2014.
45. G. Driessens, J. Kline, and T. F. Gajewski, “Costimulatory and coinhibitory receptors in anti-tumor immunity.,” *Immunol Rev*, vol. 229, no. 1, pp. 126–144, May 2009.
46. S. L. Topalian, C. G. Drake, and D. M. Pardoll, “Targeting the PD-1/B7-H1(PD-L1) pathway to activate anti-tumor immunity.,” *Curr Opin Immunol*, vol. 24, no. 2, pp. 207–212, Apr. 2012.
47. G. S. Herter-Sprie *et al.*, “Synergy of radiotherapy and PD-1 blockade in Kras-mutant lung cancer.,” *JCI insight*, vol. 1, no. 9, p. e87415, Jun. 2016.
48. K. Koikawa *et al.*, “Targeting Pin1 renders pancreatic cancer eradicable by synergizing with immunochemotherapy.,” *Cell*, vol. 184, no. 18, pp. 4753-4771.e27, Sep. 2021.
49. Z. Hu *et al.*, “Splicing Regulator p54(nrb) /Non-POU Domain-Containing Octamer-Binding Protein Enhances Carcinogenesis Through Oncogenic Isoform Switch of MYC Box-Dependent Interacting Protein 1 in Hepatocellular Carcinoma.,” *Hepatology*, vol. 72, no. 2, pp. 548–568, Aug. 2020.
50. F. D. Sigoillot and R. W. King, “Vigilance and validation: Keys to success in RNAi screening.,” *ACS Chem Biol*, vol. 6, no. 1, pp. 47–60, Jan. 2011.
51. P. Lassus, J. Rodriguez, and Y. Lazebnik, “Confirming specificity of RNAi in mammalian cells.,” *Sci STKE*, vol. 2002, no. 147, p. pl13, Aug. 2002.
52. S. Bélanger, M. Côté, D. Lane, S. L’Espérance, C. Rancourt, and A. Piché, “Bcl-2 decreases cell proliferation and promotes accumulation of cells in S phase without affecting the rate of apoptosis in human ovarian carcinoma cells.,” *Gynecol Oncol*, vol. 97, no. 3, pp. 796–806, Jun. 2005.
53. S. F. Mansilla *et al.*, “UV-triggered p21 degradation facilitates damaged-DNA replication and preserves genomic stability.,” *Nucleic Acids Res*, vol. 41, no. 14, pp. 6942–6951, Aug. 2013.
54. S. C. Gehen, P. F. Vitiello, R. A. Bambara, P. C. Keng, and M. A. O’Reilly, “Downregulation of PCNA potentiates p21-mediated growth inhibition in response to hyperoxia.,” *Am J Physiol Lung Cell Mol Physiol*, vol. 292, no. 3, pp. L716-24, Mar. 2007.
55. C. J. Sherr, “Cancer cell cycles.,” *Science*, vol. 274, no. 5293, pp. 1672–1677, Dec. 1996.

56. K. Yang, M. Hitomi, and D. W. Stacey, “Variations in cyclin D1 levels through the cell cycle determine the proliferative fate of a cell.,” *Cell Div*, vol. 1, p. 32, Dec. 2006.
57. S. Benchimol, “p53-dependent pathways of apoptosis.,” *Cell death and differentiation*, vol. 8, no. 11. England, pp. 1049–1051, Nov-2001.
58. R. Sever and J. S. Brugge, “Signal transduction in cancer.,” *Cold Spring Harb Perspect Med*, vol. 5, no. 4, Apr. 2015.
59. M. Egeblad and Z. Werb, “New functions for the matrix metalloproteinases in cancer progression.,” *Nat Rev Cancer*, vol. 2, no. 3, pp. 161–174, Mar. 2002.
60. H. Li, Z. Qiu, F. Li, and C. Wang, “The relationship between MMP-2 and MMP-9 expression levels with breast cancer incidence and prognosis.,” *Oncol Lett*, vol. 14, no. 5, pp. 5865–5870, Nov. 2017.
61. X. Wang *et al.*, “Vimentin plays an important role in the promotion of breast cancer cell migration and invasion by leucine aminopeptidase 3.,” *Cytotechnology*, vol. 72, no. 5, pp. 639–647, Oct. 2020.
62. R. A. Battaglia, S. Delic, H. Herrmann, and N. T. Snider, “Vimentin on the move: new developments in cell migration.,” *F1000Research*, vol. 7, 2018.
63. U. H. Frixen *et al.*, “E-cadherin-mediated cell-cell adhesion prevents invasiveness of human carcinoma cells.,” *J Cell Biol*, vol. 113, no. 1, pp. 173–185, Apr. 1991.
64. G. Berx *et al.*, “E-cadherin is a tumour/invasion suppressor gene mutated in human lobular breast cancers.,” *EMBO J*, vol. 14, no. 24, pp. 6107–6115, Dec. 1995.
65. X. Li *et al.*, “Intrinsic resistance of tumorigenic breast cancer cells to chemotherapy.,” *J Natl Cancer Inst*, vol. 100, no. 9, pp. 672–679, May 2008.

Figures

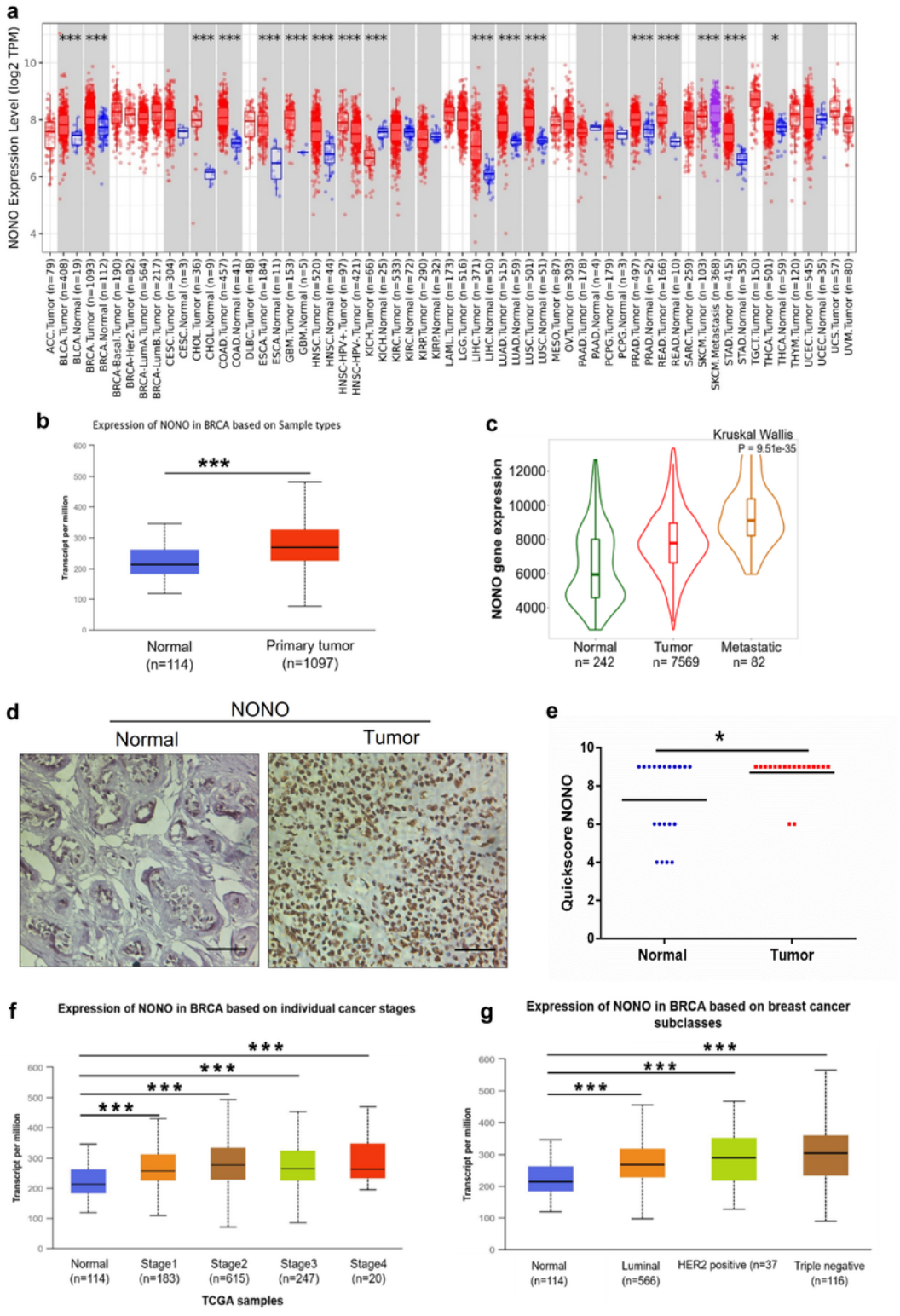

Figure 1

NONO is significantly expressed in breast cancer. a Expression levels of NONO in various cancers and their respective normal tissues according to data retrieved from the TIMER database. **b** TCGA data from UALCAN suggested that NONO expression was significantly higher in breast cancer than normal breast tissues. **c** NONO gene expression profile in normal breast tissues, breast tumor, and metastatic breast tissues. Using TNMplot web platform. **d** Representative IHC image of NONO protein expression in breast

cancer tissue and adjacent normal tissue. Scale bar, 50 μm. **e** Quickscore distribution of NONO in breast cancer tissues (n = 20) versus normal tissue (n = 20). **f, g** According to TCGA data from UALCAN, NONO is significantly overexpressed in different stages and subclasses of breast cancer. *p<0.05, ***p<0.001.

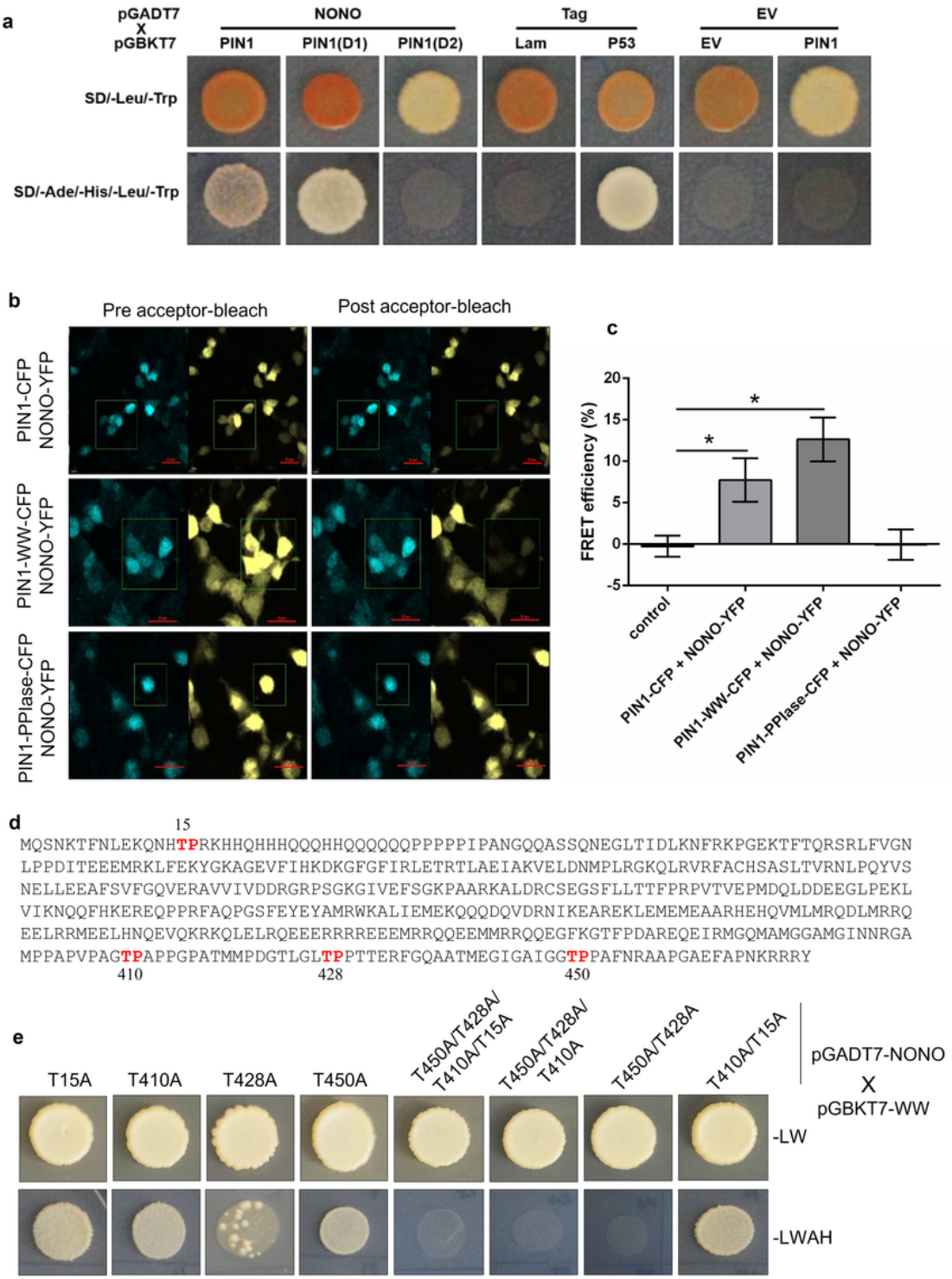

Figure 2

C-terminal thr-pro motifs in NONO specifically interact with the WW domain of PIN1. a Yeast two-hybrid analysis shows the protein-protein interactions of NONO with PIN1 and PIN1-WW domain. The yeast strains containing bait and prey plasmids were mated. The diploids were selected on double-dropout media –LT (SD-Leu/-Trp) and quadra-dropout media –LTHA (SD/-Leu/-Trp/-Ade/-His) for yeast two-hybrid screening. P53-BD/T antigen-AD and Lam-BD/T antigen-AD were used as positive and negative controls. **b** Detection of FRET by acceptor photobleaching. HEK293T cells were co-transfected with PIN1-CFP/NONO-YFP, PIN-WW-CFP/NONO-YFP, PIN1-PPIase-CFP/NONO-YFP. After 48 hours of transfection, the cells were fixed, the images of CFP and YFP were taken using CFP and YFP channels, and the intensities were measured before and after acceptor photobleaching. scale bar 25 μm **c** The bar graph representing FRET efficiency of various cyan/yellow pairs. Data are presented as mean ± standard deviation with n ≥ 3.p*<0.05. **d** Presence of four the-pro motifs in NONO ORF (CCDS14410.1). *Source*: The National Centre for Biotechnology Information (https://www.ncbi.nlm.nih.gov/). **e**Site-directed mutagenesis identifies the thr-pro motifs essential for the interaction of NONO with the PIN1-WW domain. The effect of substituting threonine with glycine at thr-pro motifs within NONO ORF was analyzed by yeast-two hybrid screening. The two thr-pro motifs at the C-terminal of NONO are critical for the interaction of NONO with the PIN1-WW domain.

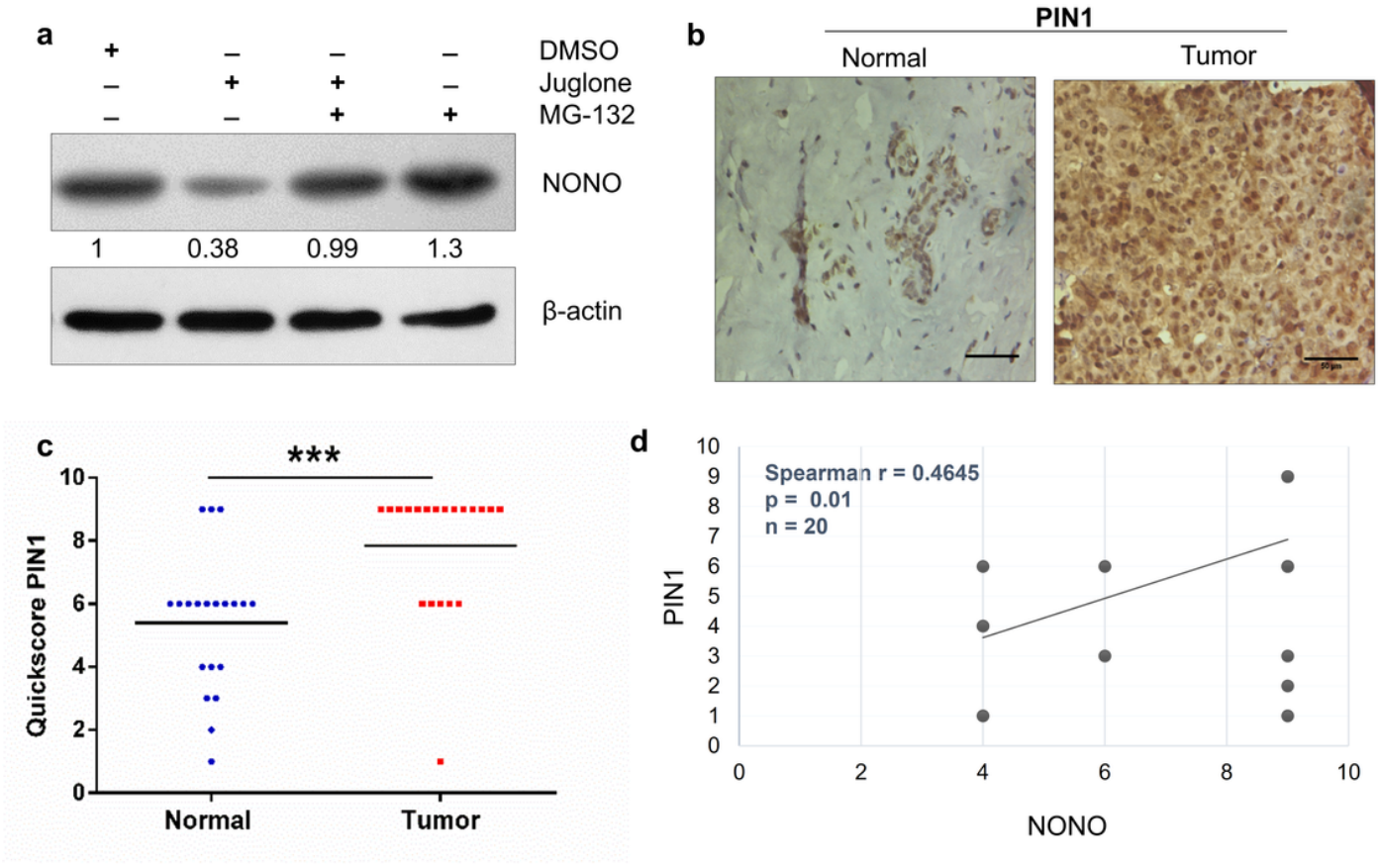

Figure 3

The stability of NONO protein is enhanced by PIN1. a MDA-MB-231 cells were treated with Juglone or DMSO. About 48 hours later, cells were further treated with MG132 for 8 hours. Western blotting analysis revealed the involvement of PIN1 in the abundance and regulation of NONO protein via the proteasomal inhibition pathway. β-actin was used as an internal control and ImageJ software for densitometry analysis. **b** Representative IHC image of PIN1 protein expression in breast tumor and normal tissues. Scale bar, 50 μm. **c** Distribution of PIN1 IHC signals in breast versus normal tissues was analyzed by quick score method. Unpaired Mann Whitney test was used to compare IHC quick scores in tumor versus normal tissues. **d** Significant association (Spearman's rank correlation coefficient r = 0.464, *p* = 0.01, n = 20) between NONO and PIN1 proteins was observed in breast cancers. p*<0.05, ***p<0.001.

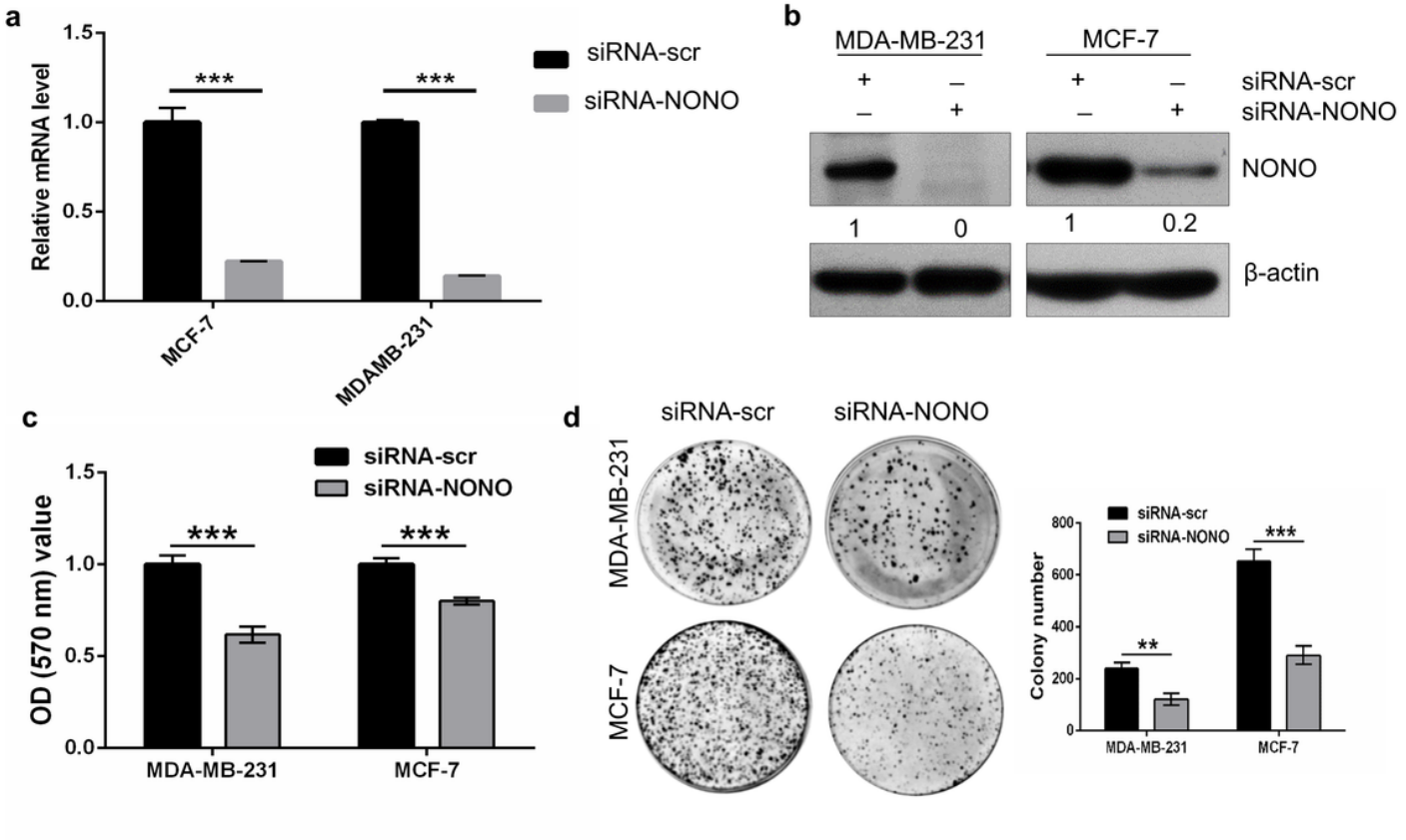

Figure 4

Silencing of NONO inhibits the tumorigenesis and colony formation ability of MDA-MD-231 and MCF-7 breast cancer cells. a, b siRNA-NONO is efficient in knocking down the NONO gene at the transcription level and the corresponding protein level as demonstrated by RT-PCR and western blotting, respectively. **c** crystal violet assay demonstrated the proliferation ability of breast cancer cells transfected with siRNA-NONO and siRNA-scr. **d** The clonogenicity of NONO silenced breast cancer cells was determined by colony formation assay. Bars show the mean ± SD of at least triplicates. **p<0.01, ***p<0.001.

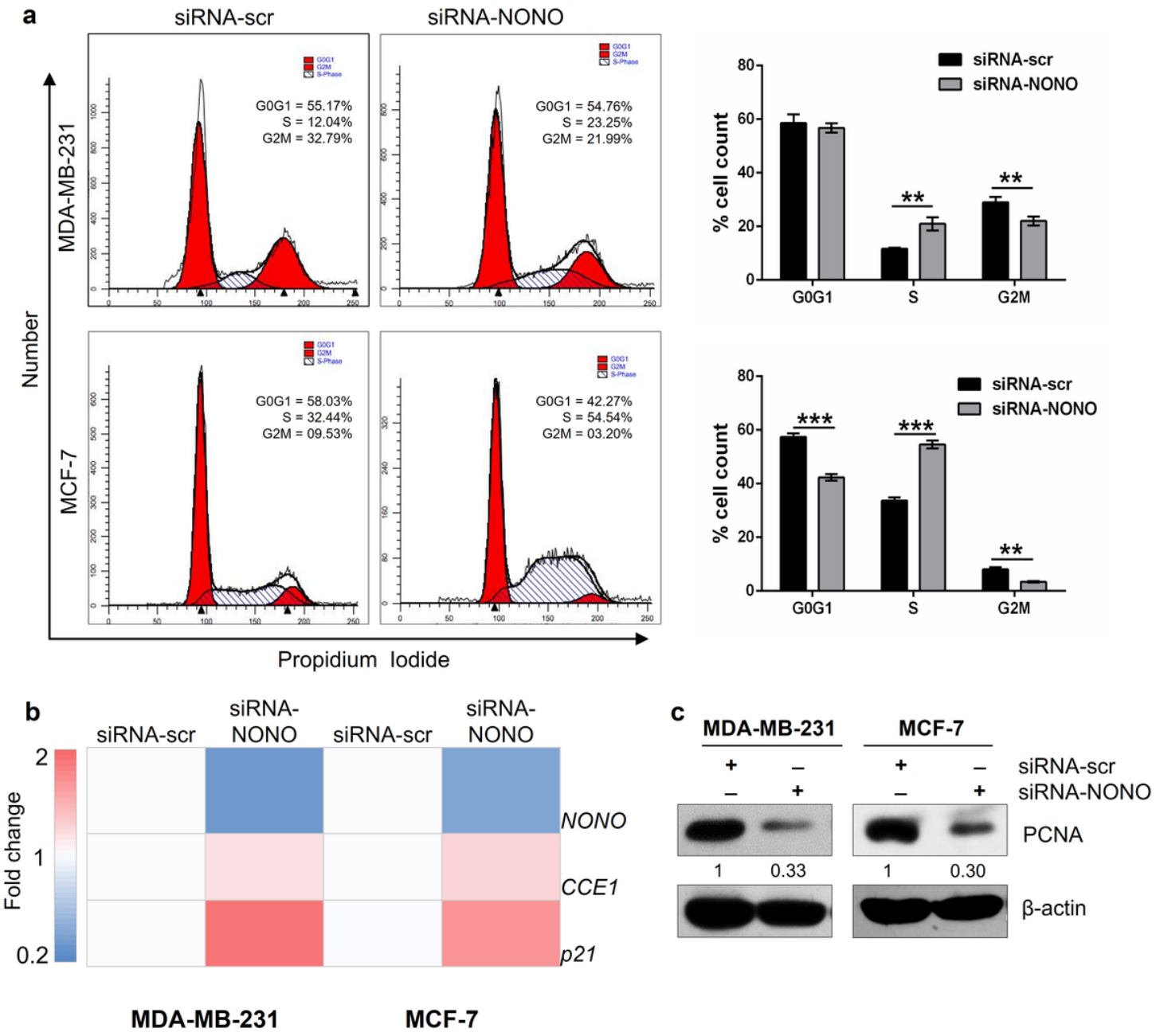

Figure 5

Silencing of NONO gene expression induces S-phase cell cycle arrest in MDA-MB-231 and MCF-7 breast cancer cells. asilencing of NONO induced the accumulation of cells in the S phase, as revealed by flow cytometry. **b** Quantification of cell cycle regulatory genes using qRT-PCR in MDA-MB-231 and MCF-7 cells. NONO silencing affects the expression of cell cycle-related genes. CCE1 (cyclinE) was significantly downregulated whereas CDKN1A (P21) was highly upregulated in MDA-MB-231 and MCF-7 breast cancer cells. **a, b** Data represented as mean ± SD of three independent experiments. p*<0.05, **p<0.01, ***p<0.001. **c** Western blot analysis of PCNA in control and NONO silenced MDA-MB-231 and MCF-7 cells. The expression of PCNA was inhibited in both the cell lines. β-actin has been used as an internal control, ImageJ software for densitometry analysis.

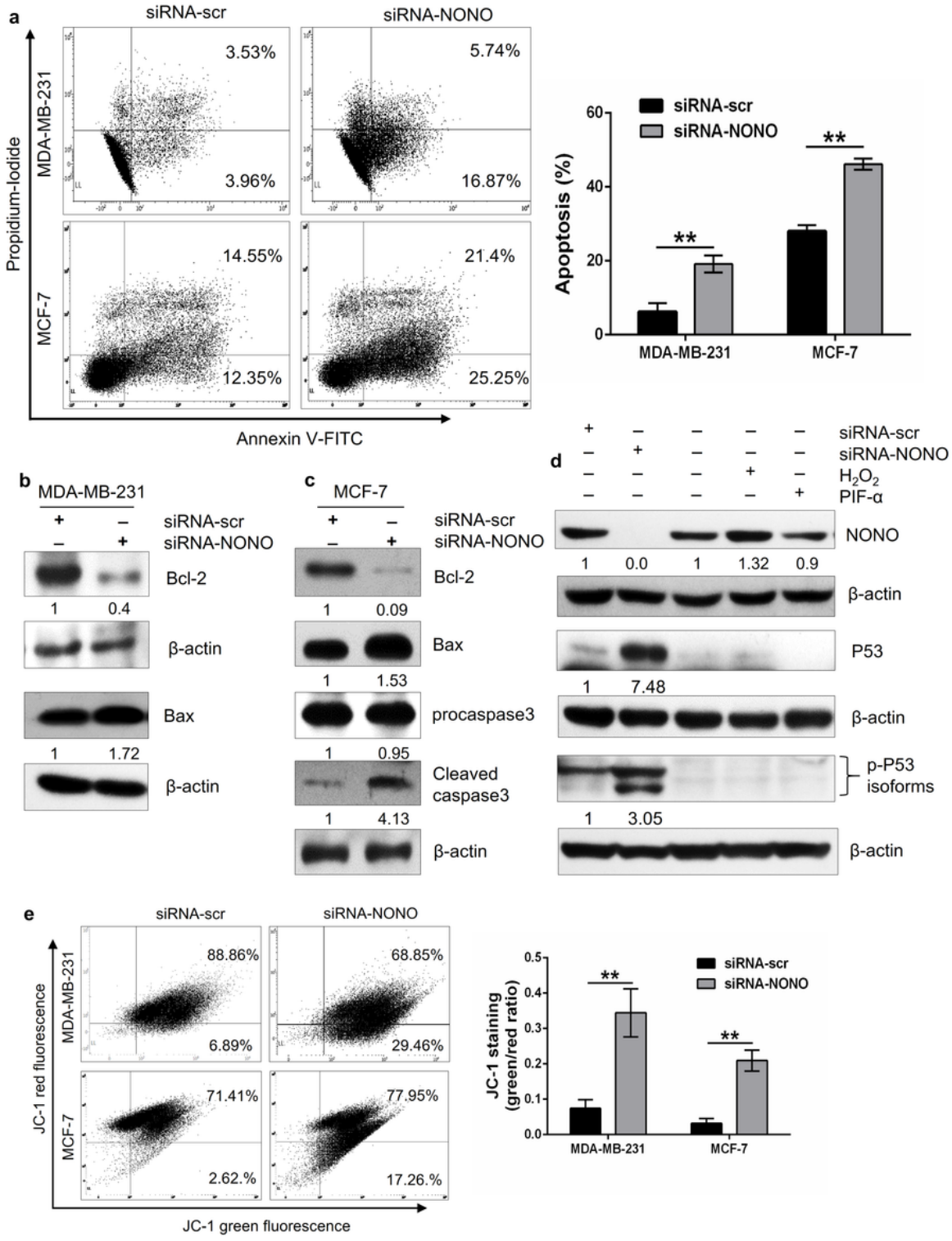

Figure 6

Silencing of NONO induces apoptosis in MDA-MB-231 and MCF-7 cells. **a** PI and annexin V staining of NONO depleted MDA-MB-231, and MCF-7 cells were determined by flow cytometry after 72 hours of transfection. The percentage of apoptotic cells was plotted for MDA-MB-231 and MCF-7 cells. **p<0.01. **b, c** The expression of Bcl-2 and Bax in MDA-MB-231 and MCF-7, and procaspase-3 and cleaved caspase 3 in MCF-7 was analyzed by Western blot analysis. **d** Expression of apoptotic proteins p53 and p-p53 in

NONO depleted MCF 7 cells. Treatment of H_2O_2 with 50 μM for 6 hours promotes expression of NONO, while the treatment of p53 inhibitor PIF-α for 24 hours does not affect NONO expression. **e** The effect of NONO silencing on the change of mitochondrial membrane potential (MMP) by JC-1. **a, e** Data represented as mean ± SD of three independent experiments. **p<0.01. **b, c, d** Representative blots are shown from at least two independent experiments. β-actin was used as an internal control.

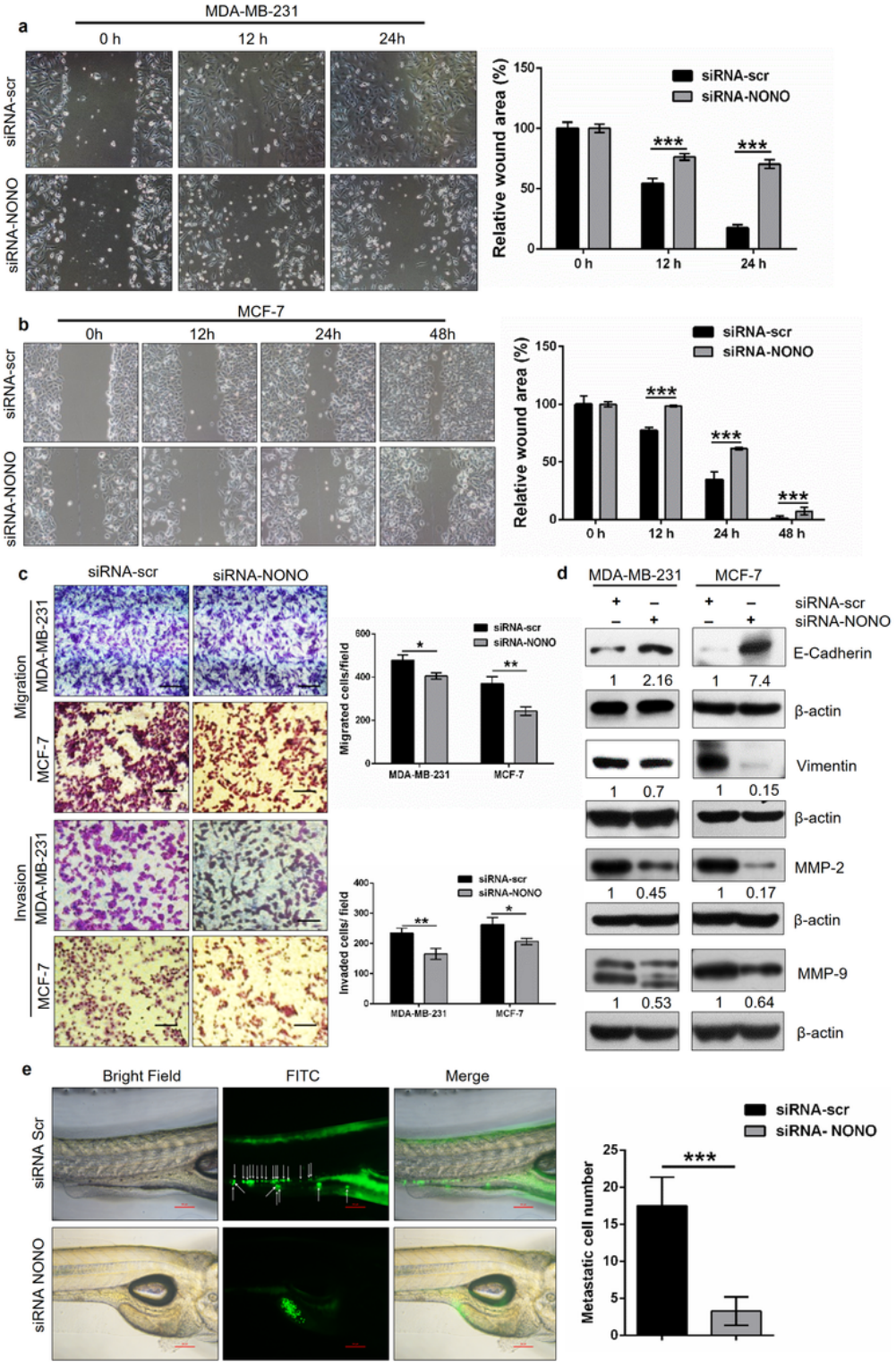

Figure 7

NONO knockdown inhibits the migration and invasion potential of breast cancer cells *invitro* and *in vivo*. **a, b** The migratory capacity of siRNA-scr and siRNA-NONO transfected breast cancer cells was investigated using a wound-healing assay. ImageJ 64 was used to measure wound area. Magnification, 10X. **c** The transwell migration and invasion assay determined the migration and invasion capacities of MDA-MB-231 and MCF-7 breast cancer cells transfected with siRNA-scr and siRNA-NONO. Scale bar, 100 µm and magnification, 20X. **a-c,** the data is the representation of three independent experiments. *p<0.05, **p<0.01, p***<0.001. **d** Western blot analysis of the expression of E-cadherin, Vimentin, MMP-2, and MMP-9 proteins in the siRNA-scr and siRNA-NONO transfected breast cancer cells. β-actin served as a protein loading control. The epithelial marker E-cadherin was upregulated, and mesenchymal marker vimentin was downregulated in NONO knockdown cells. Endogenous MMP-2 and MMP-9 expression levels were decreased by NONO knockdown. Representative blots are shown from at least two independent experiments. β-actin was used as an internal control. **e** The migration of siRNA-scr and siRNA-NONO transfected MDA-MB-231 cells was studies by staining the cells with Green CMFDA and injected into the perivitelline space of 48 hpf zebrafish wild-type embryos and the images were captured using fluorescence microscope, as described in the material and methods section. The number of migrated cells per zebrafish embryo was counted manually using FIJI software. Representative images of 72 h after injection are shown. Scale bar, 100 µm and magnification, 10X. The graph represents the mean ± SD from n > 25 embryos. Statistical analysis was performed using non-parametric two-tailed Mann-Whitney *U*-test.

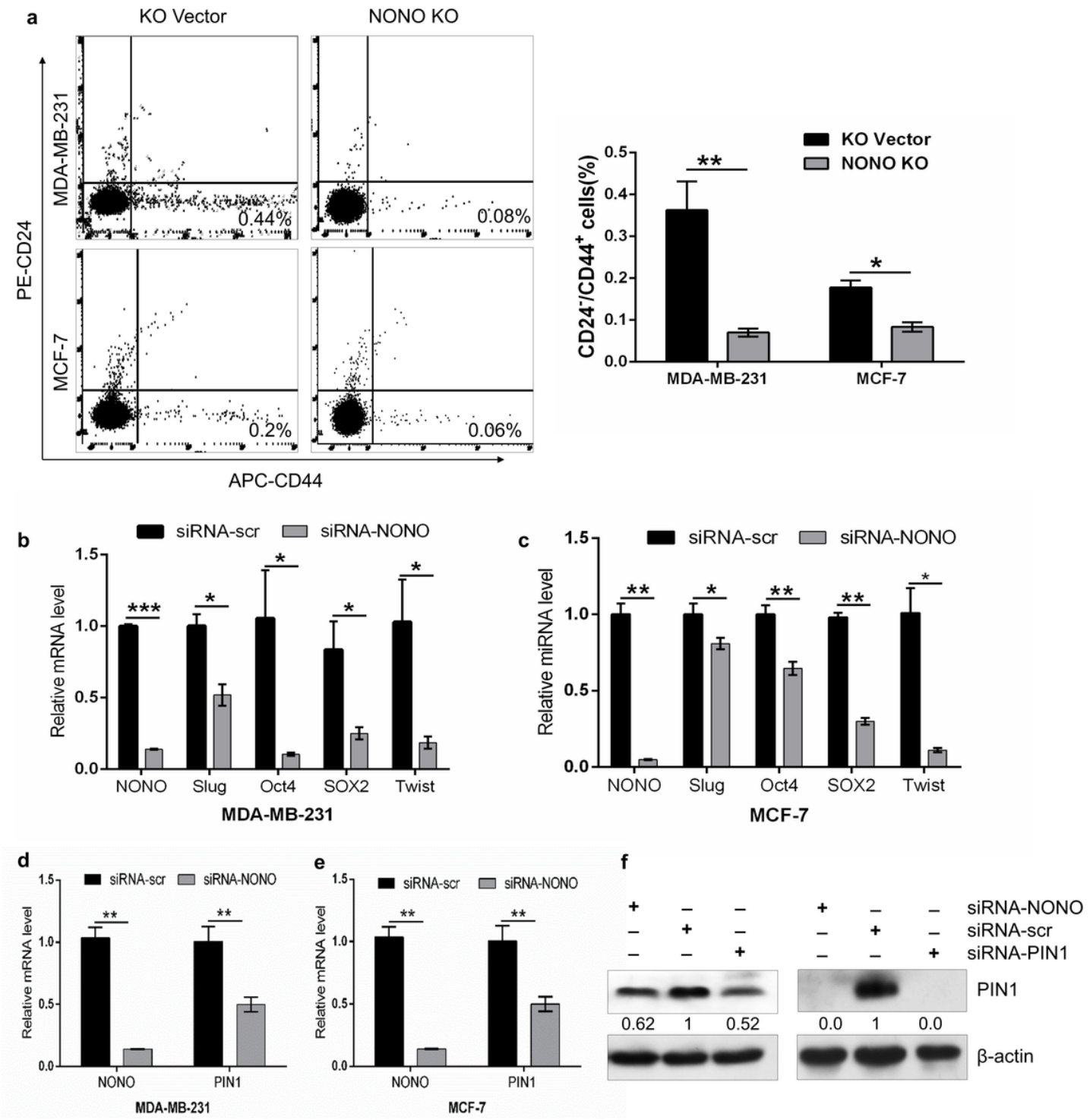

Figure 8

NONO depletion inhibits the cancer stem cell formation in breast cancer cells. **a** FACS measured the subpopulation of the cells with CD24 $^{-}$/CD44 $^{+}$ phenotype in MDA-MB-231 and MCF-7 cells. The bar graph depicts the quantification of CD24 $^{-}$/CD44 $^{+}$ cells. **b, c** qRT-PCR expression analysis of stemness associated markers, including SLUG, OCT4, SOX2, Twist in MDA-MB-231 and MCF-7 cells. Data represented as mean ± SD of three independent experiments. **d, e** Quantification of expression of NONO and PIN1 in NONO depleted MDA-MB-231, and MCF-7 cells were analyzed by qPCR. **f** Western blotting

analysis of NONO and PIN1 protein in NONO and PIN1 depleted MDA-MB-231 and MCf-7 ells. β-actin was used as a control for equal loading and ImageJ software for densitometry analysis. **a-e** Data represented as mean ± SD of three independent experiments. ***p< 0.001, p**< 0.01, *p<0.05.

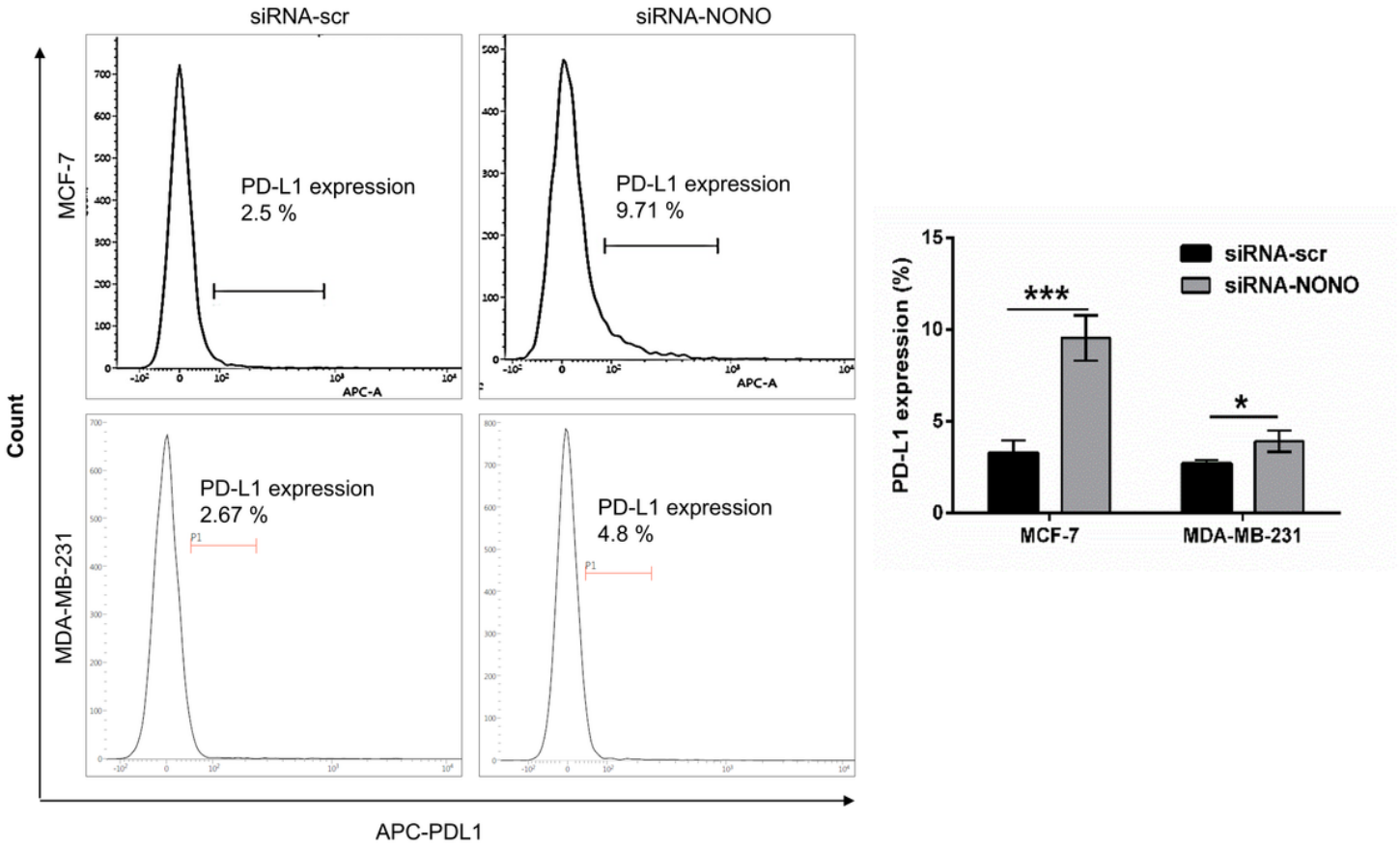

Figure 9

NONO inhibits the expression of PD-L1 in breast cancer cells. Silencing of NONO promotes the expression of PD-L1 protein at the surface of MDA-MB-231 and MCF-7 breast cancer cells. Bar plots represented as mean ± SD of three independent experiments. ***p< 0.001, *p<0.05.

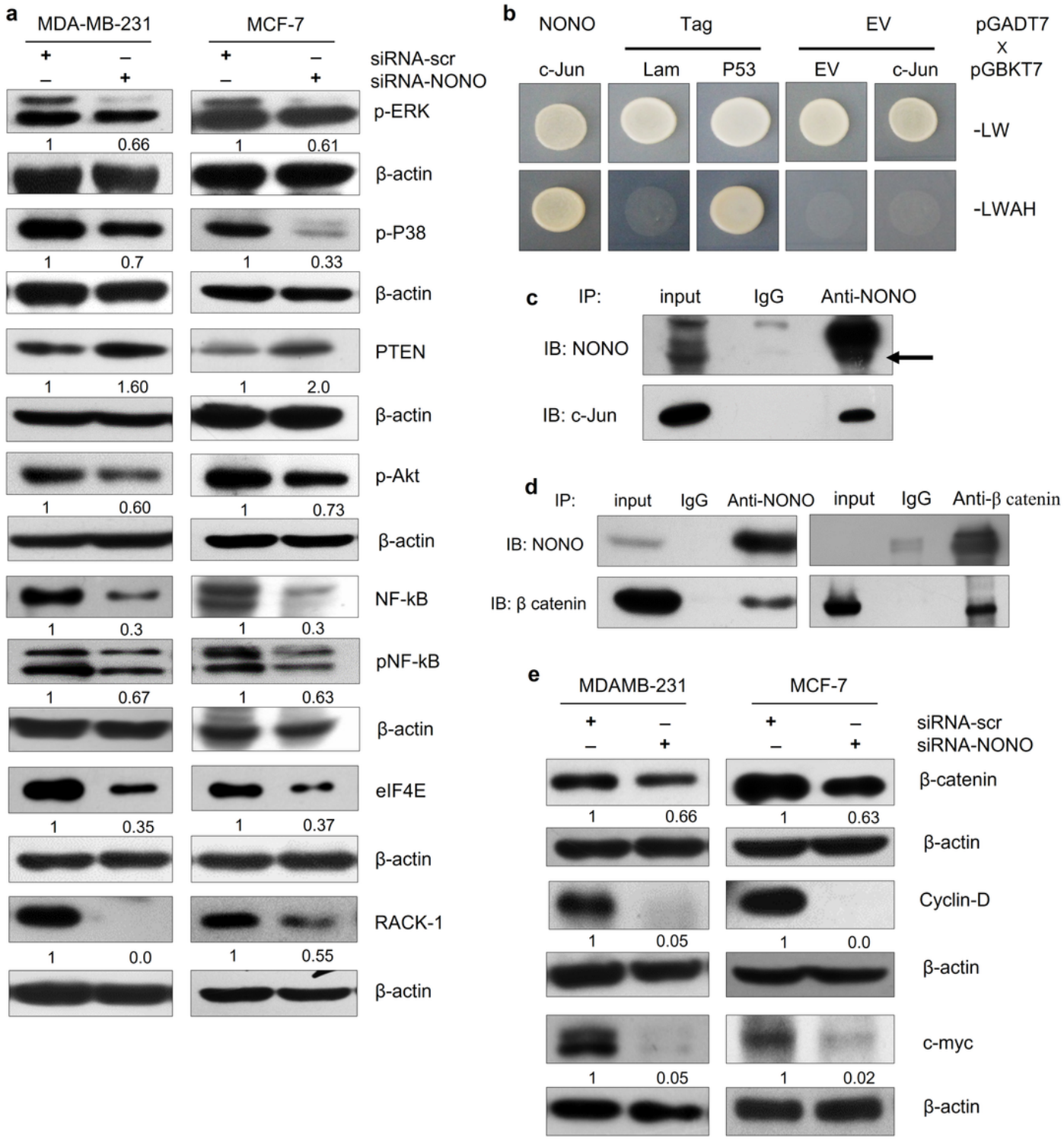

Figure 10

NONO activates MAPK/β-catenin signalling pathway in breast cancer cells. a *Total cellular protein (50 μg) from siRNA transfected MDA-MB-231 and MCF-7 cells were analyzed by western blotting with Akt/MAPK antibodies against the proteins as specified.* ***b, c*** *The interaction of NONO and c-Jun was investigated by yeast two-hybrid and immunoprecipitation/western blotting.* ***d*** *The immunoprecipitated complex of MDA-MB-231 cell lysates with anti-NONO or anti-β-catenin antibody analyzed by western blotting (IB).*

e*Silencing of NONO in MDA-MB-231 and MCF-7 cells suppresses β-catenin and the related downstream molecules such as c-myc and cyclin D1.* ***a, e*** *Representative blots are shown from two independent experiments. β-actin was used as a control for equal loading and ImageJ software for densitometry analysis.*

Supplementary Files

This is a list of supplementary files associated with this preprint. Click to download.

- SupplementaryRAWdata.pdf
- Supplementaryinformation.docx